# Diagnostics from UV spectra of low redshift quasars

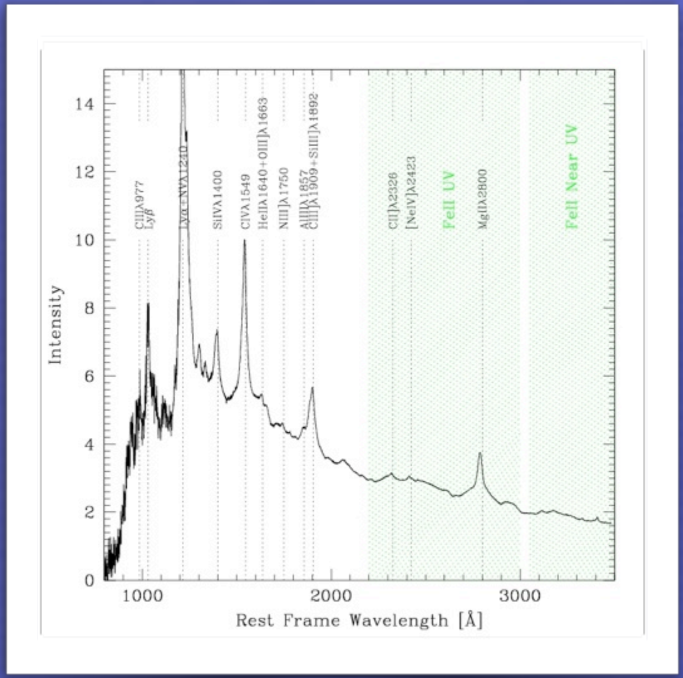


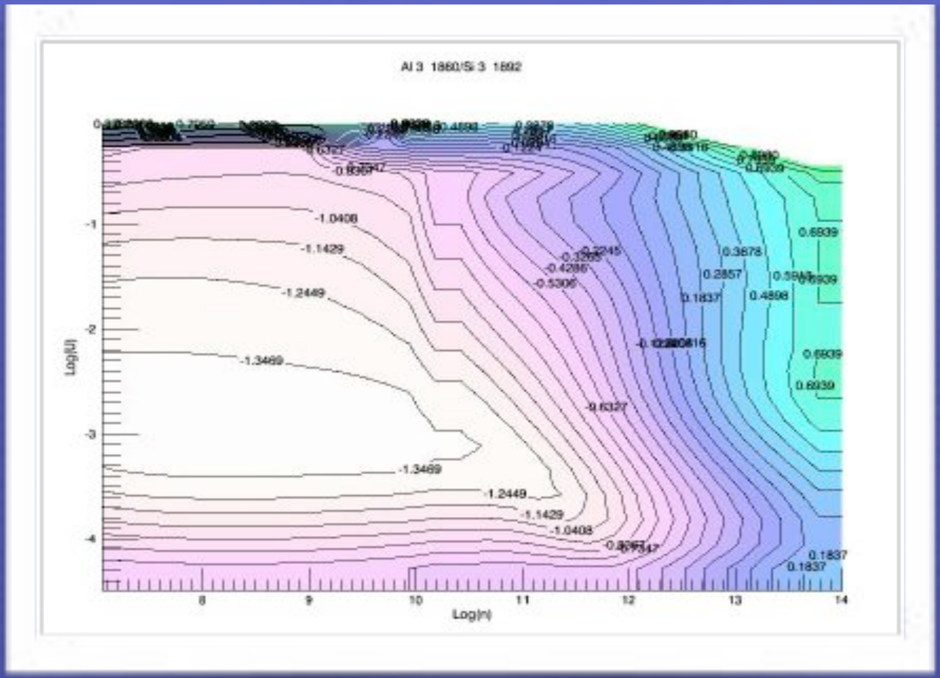


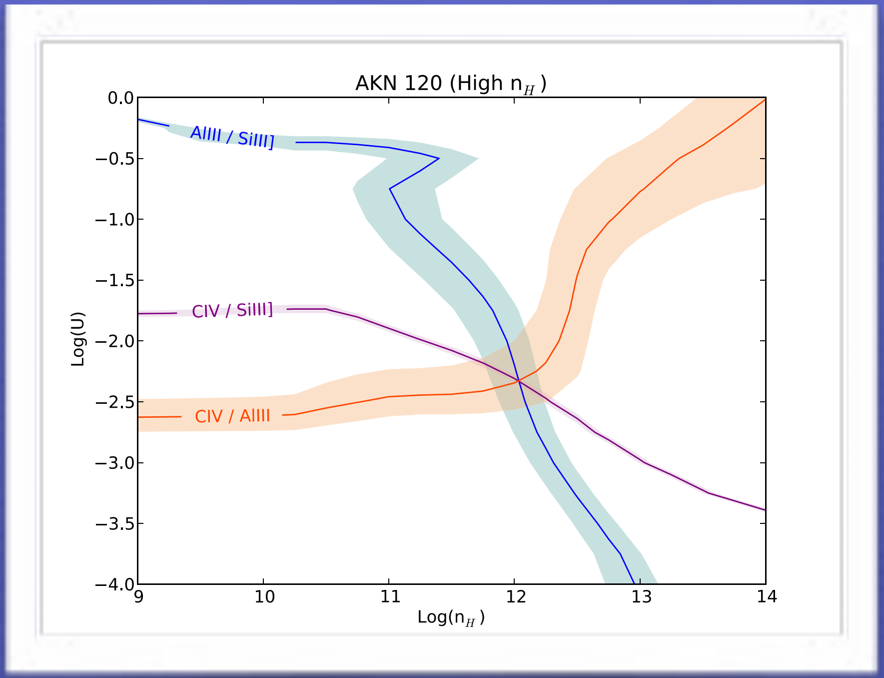



***Paola Marziani***, *INAF, Osservatorio Astronomico di Padova*

***Jack W. Sulentic*** *(IAA-CSIC)*, ***Deborah Dultzin*** *(IA-UNAM)*, ***Giovanna M. Stirpe*** *(INAF, OA Bologna)*, ***Sebastian Zamfir*** *(U. of Wisconsin)*, ***C. Alenka Negrete*** *(INAOE)*, ***Ascensión del Olmo*** *(IAA-CSIC)*, ***Mary Loli Martínez Aldama*** *(IA-UNAM , Ph. D. student)*

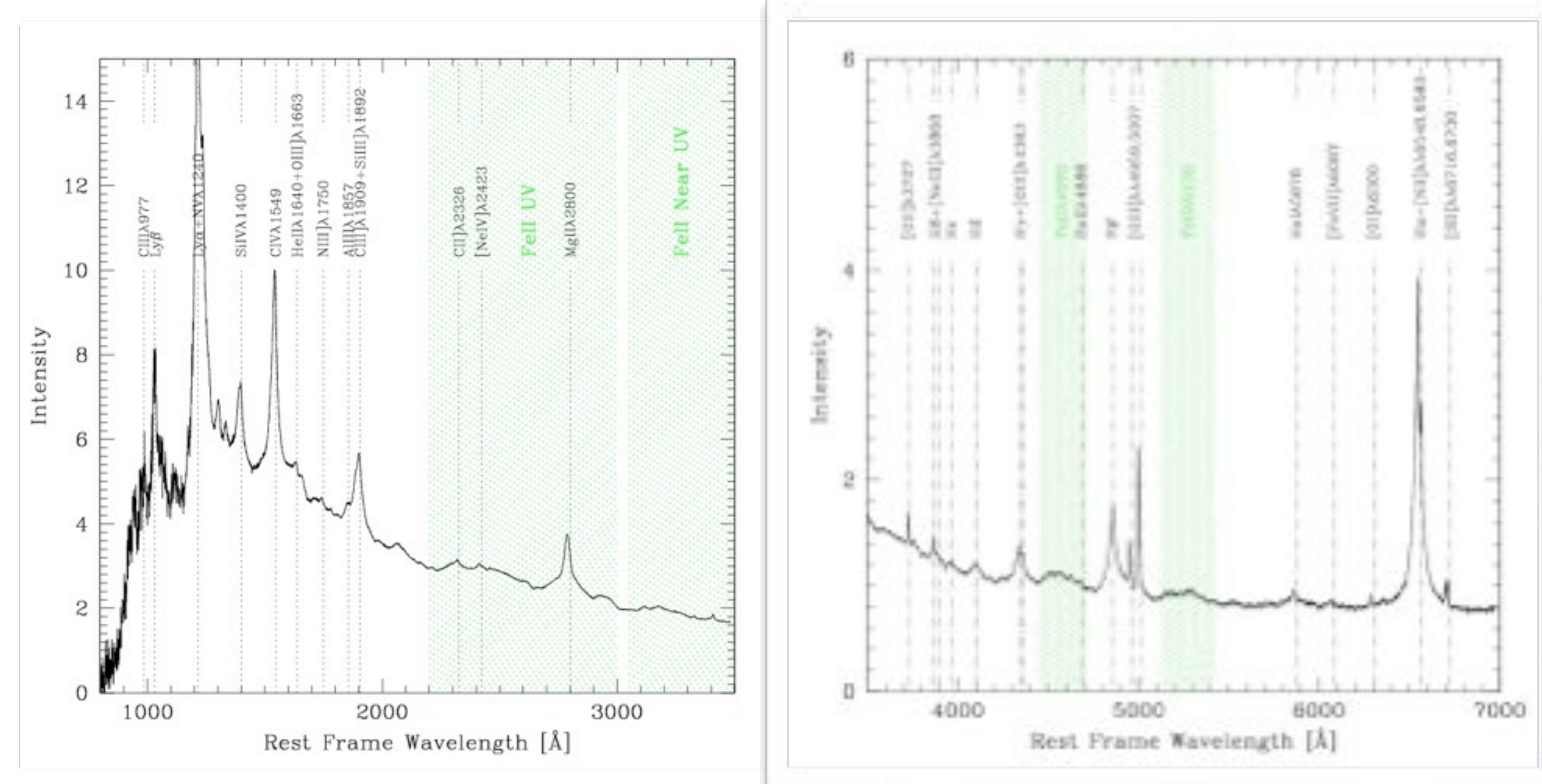


The composite rest-frame quasar spectrum from the Sloan DSS (Van den Berk et al. 2001)

# Distinctive emission line spectrum with prominent broad lines due to resonant and intercombination transitions from a spatially unresolved "broad line region" (BLR)

# Quasars do not show the same spectrum!

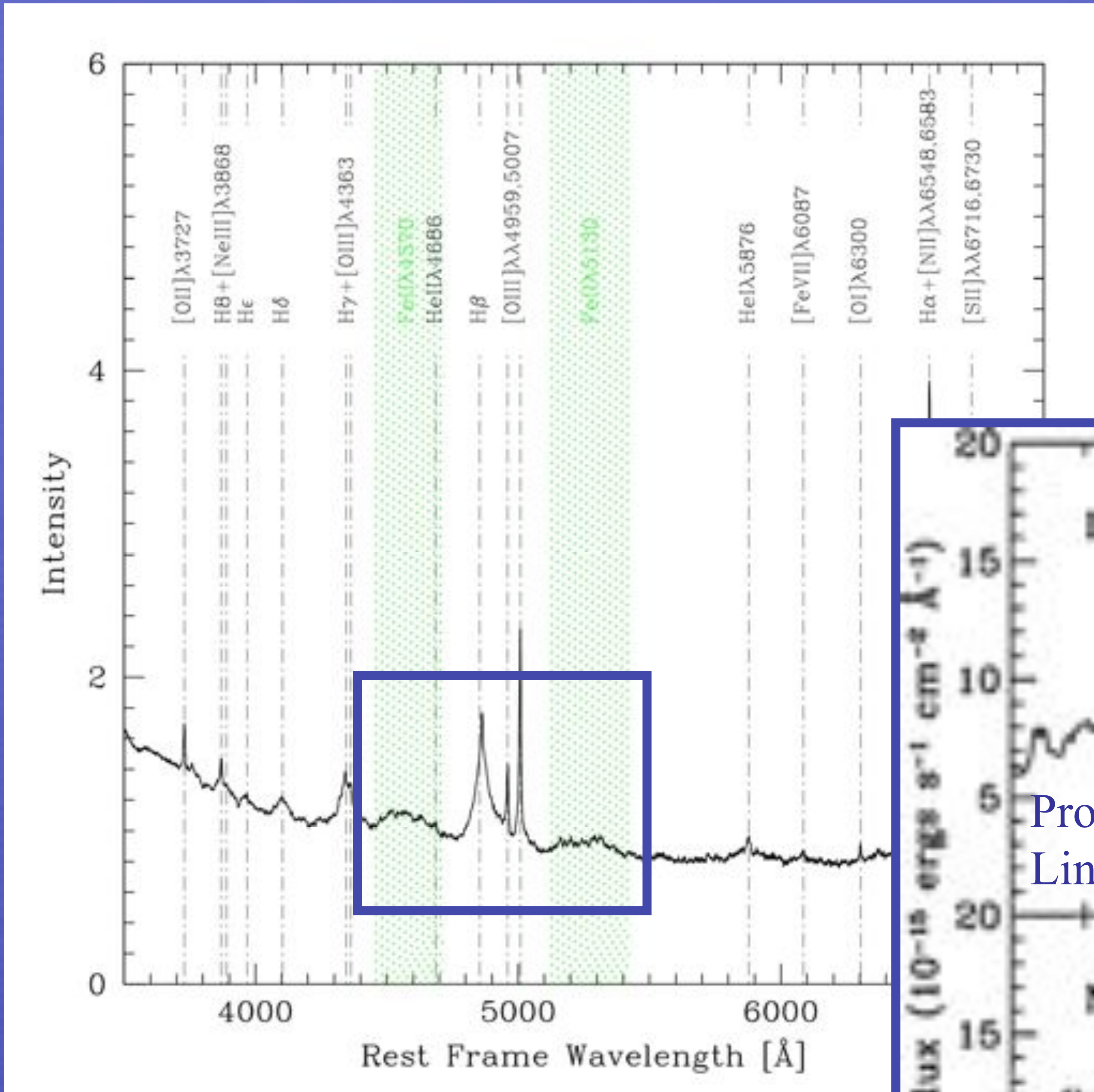


Sulentic et al. 2000

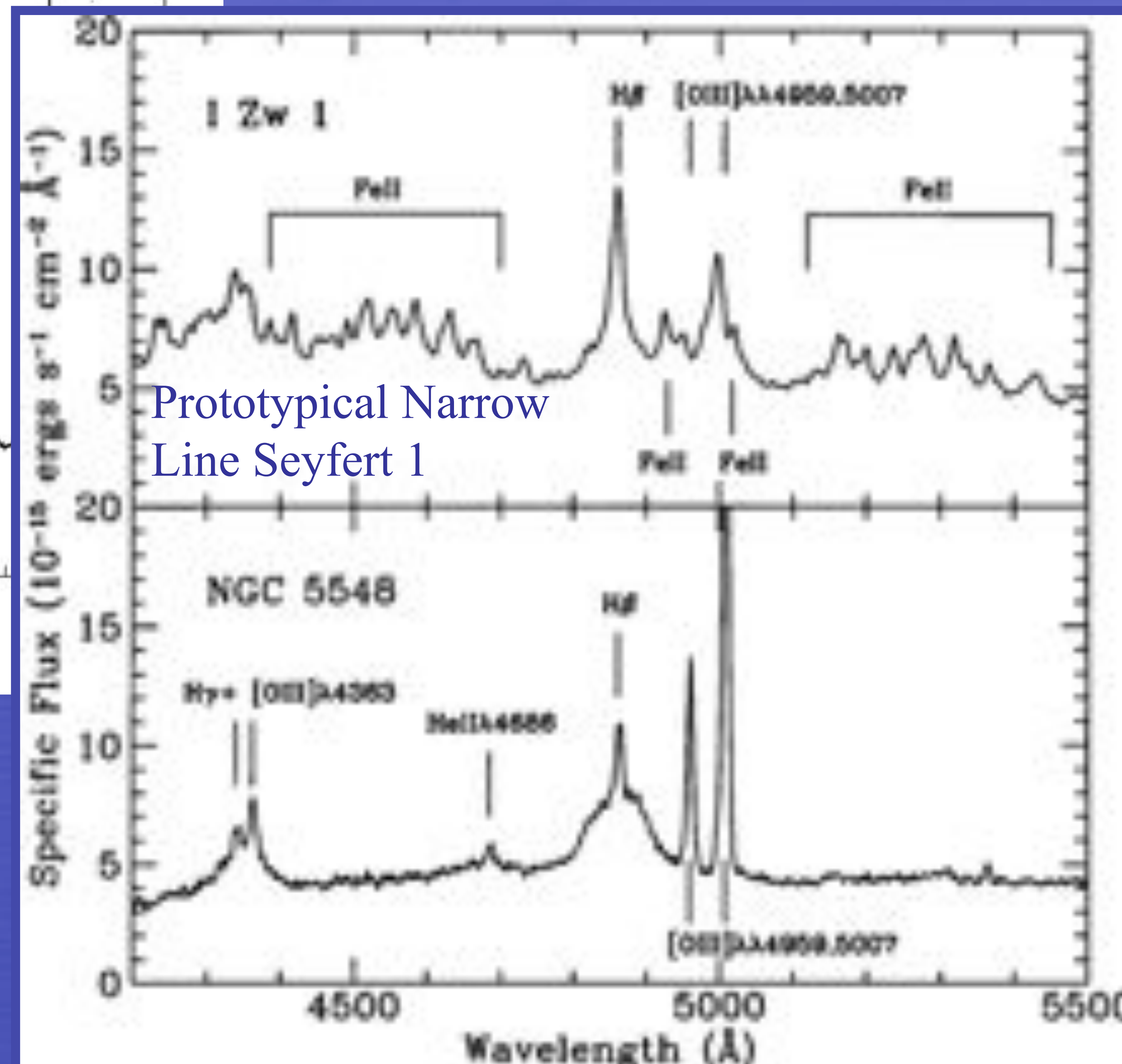


The emitting regions of these two sources are in different physical and dynamical conditions!

# Organizing quasar spectral diversity: Quasars' Eigenvector 1

Boroson & Green 1992; see also Gaskell et al. 1999

- Originally defined by a Principal Component Analysis of PG quasars.

- E1 is dominated by an anticorrelation between 1) strength of FeII$\lambda$4570, 2) width of H$\beta$.

- E1 is very robust since:

  a) found in several independent samples;

  (Dultzin-Hacyan et al. 1997; Shang et al. 2003, Yip et al.2004, Sulentic et al. 2000, 2007, Kovacevic et al. 2010, Kruzcek et al 2011, Tang et al. 2012)

  b) found for high dimension parameter spaces.

  (Kuraszkiewicz et al. 2008; Mao et al. 2009; Grupe 2004, Wang et al. 2006; Bachev et al. 2004; Sulentic et al. 2007)

The 4DE1 of Sulentic et al. includes:

3) CIV$\lambda$1549 line shift; 4) soft-X ray photon index.

# Optical plane of Eigenvector 1

## 1D sequence of spectral types to account for quasars' diverse properties at $z$<0.7

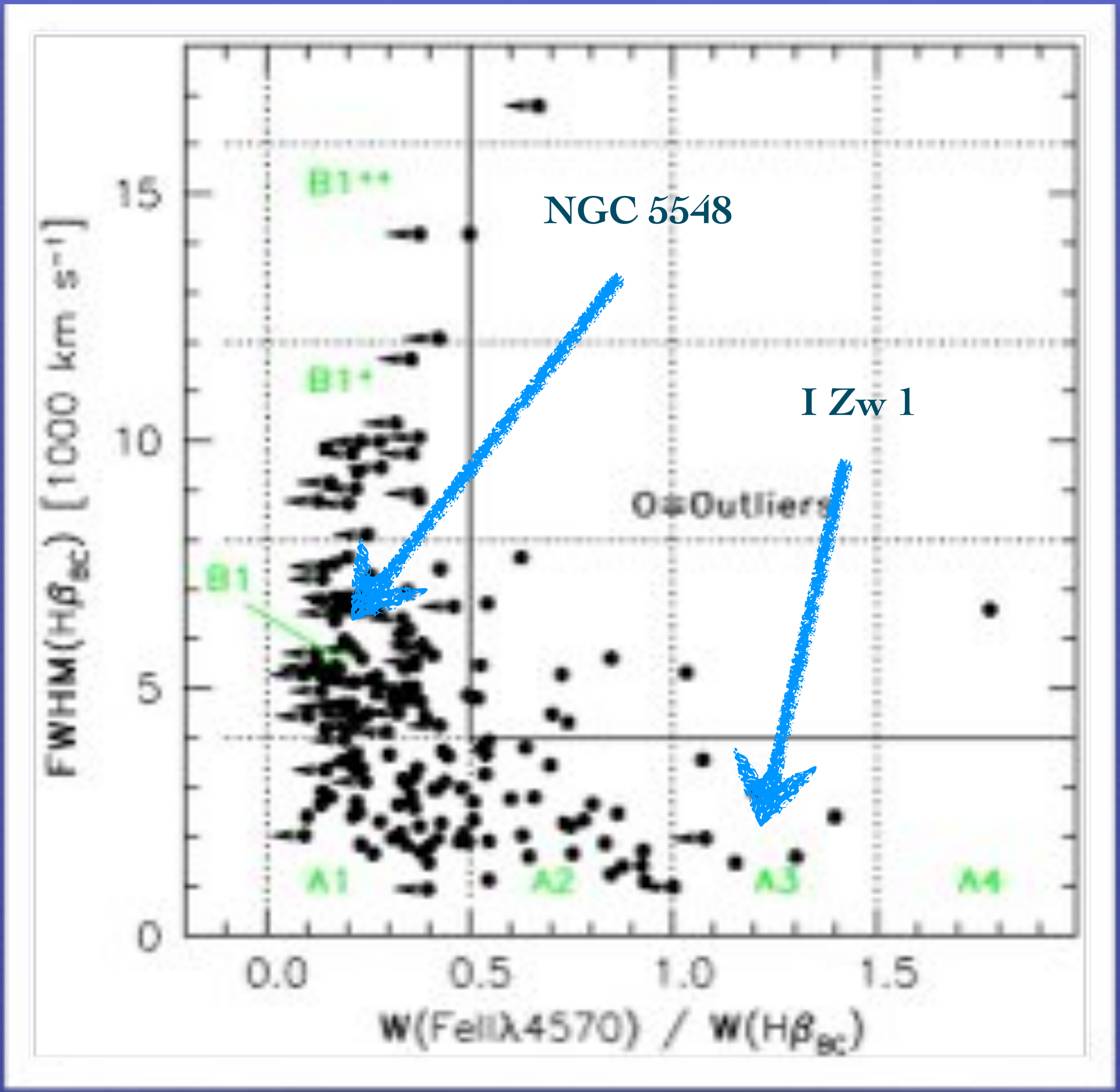


Sulentic et al. 2002

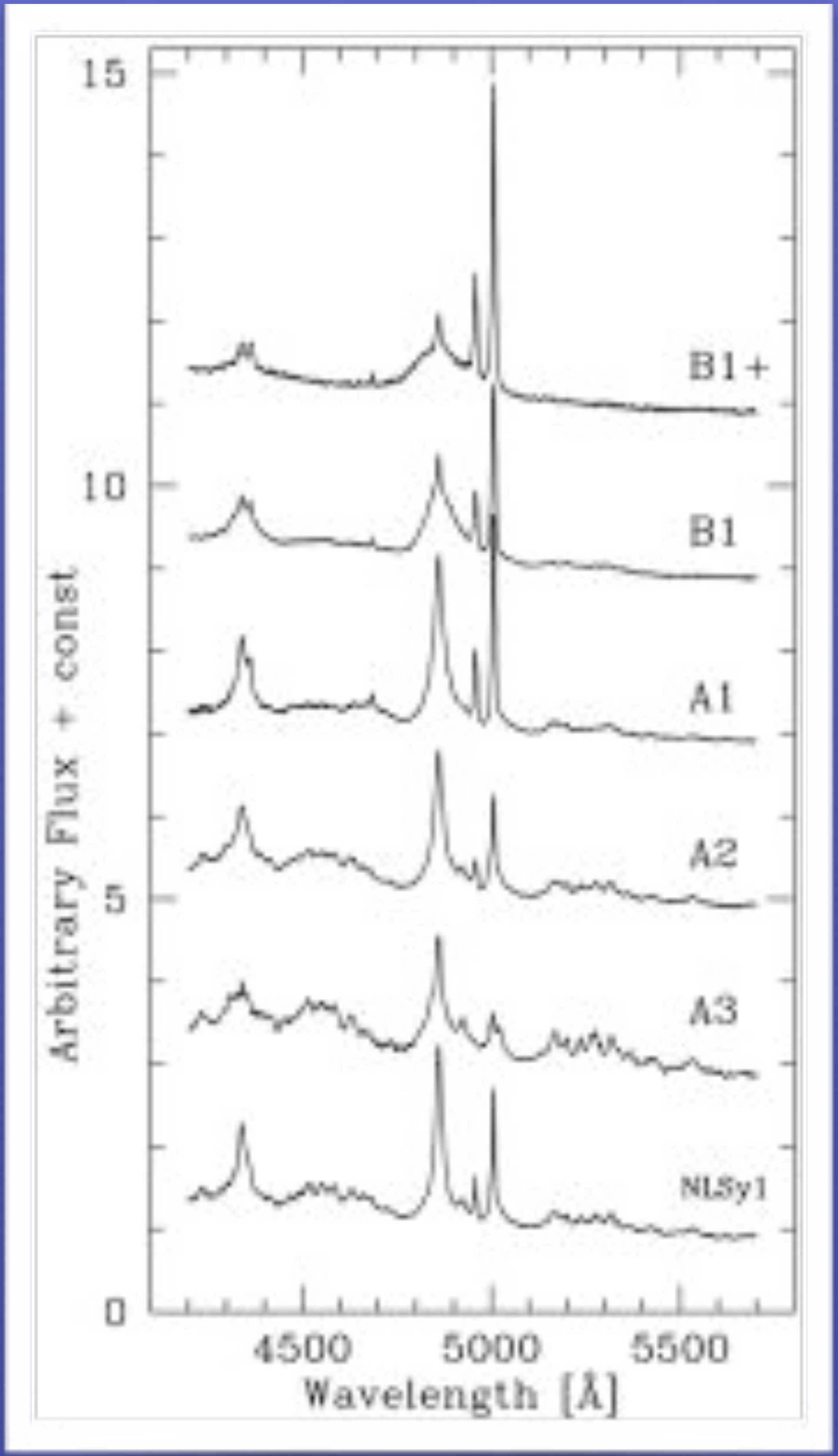

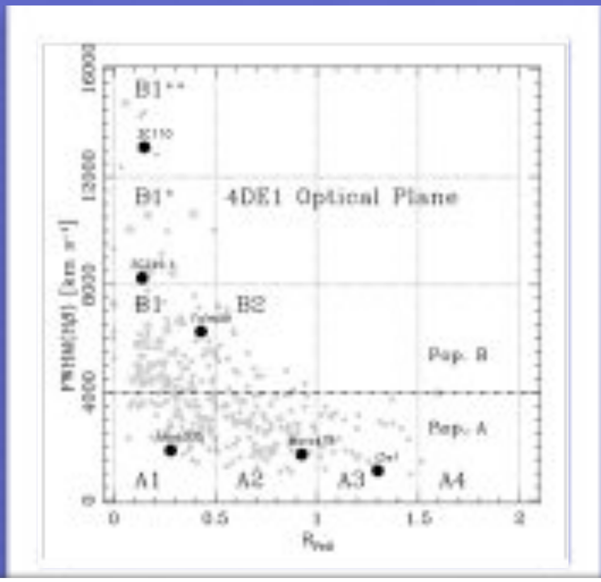


# UV spectral changes along E1

Bachev et al. 2004

## HST/FOS composite spectra of quasars at $z<0.7$

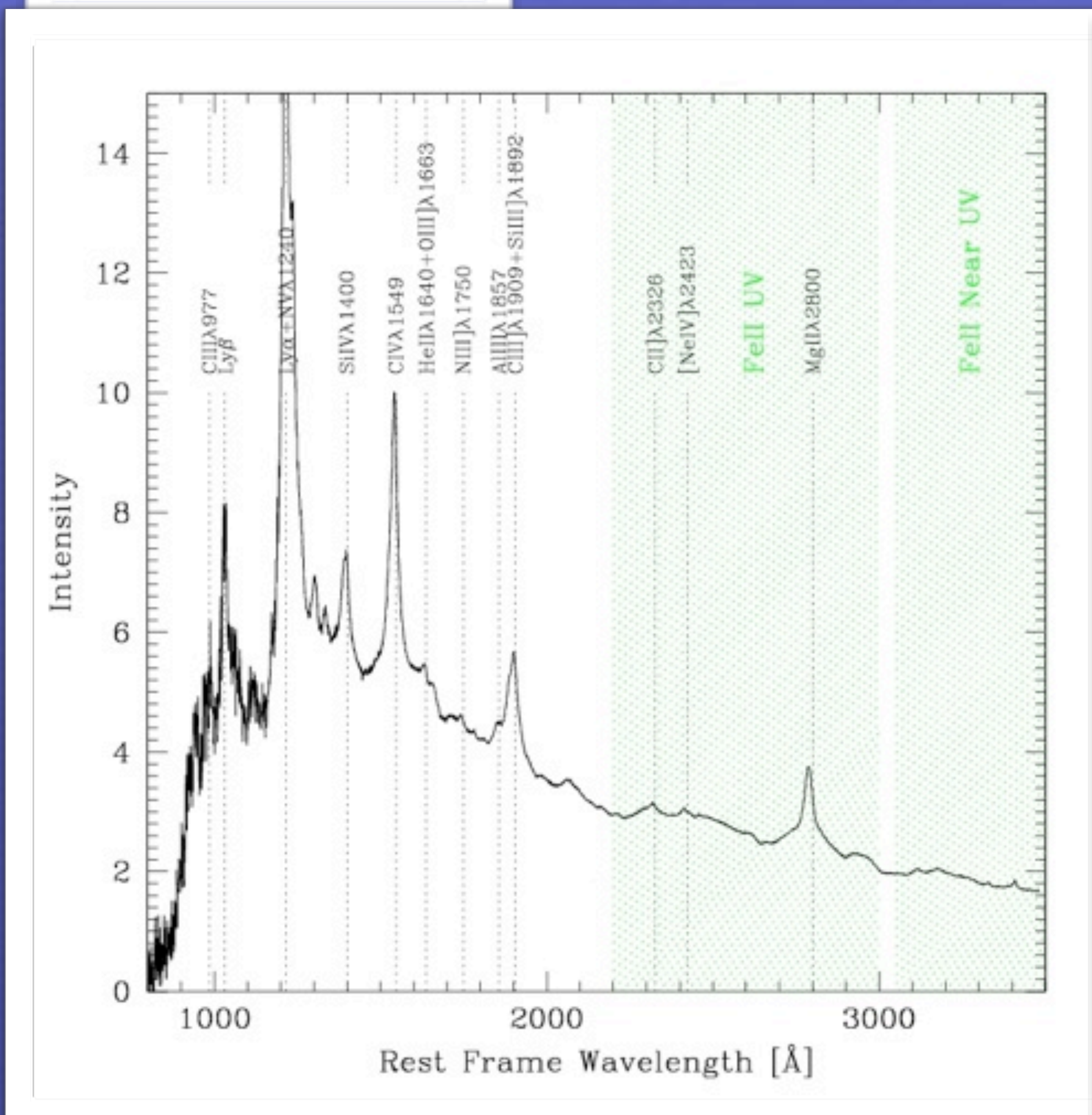


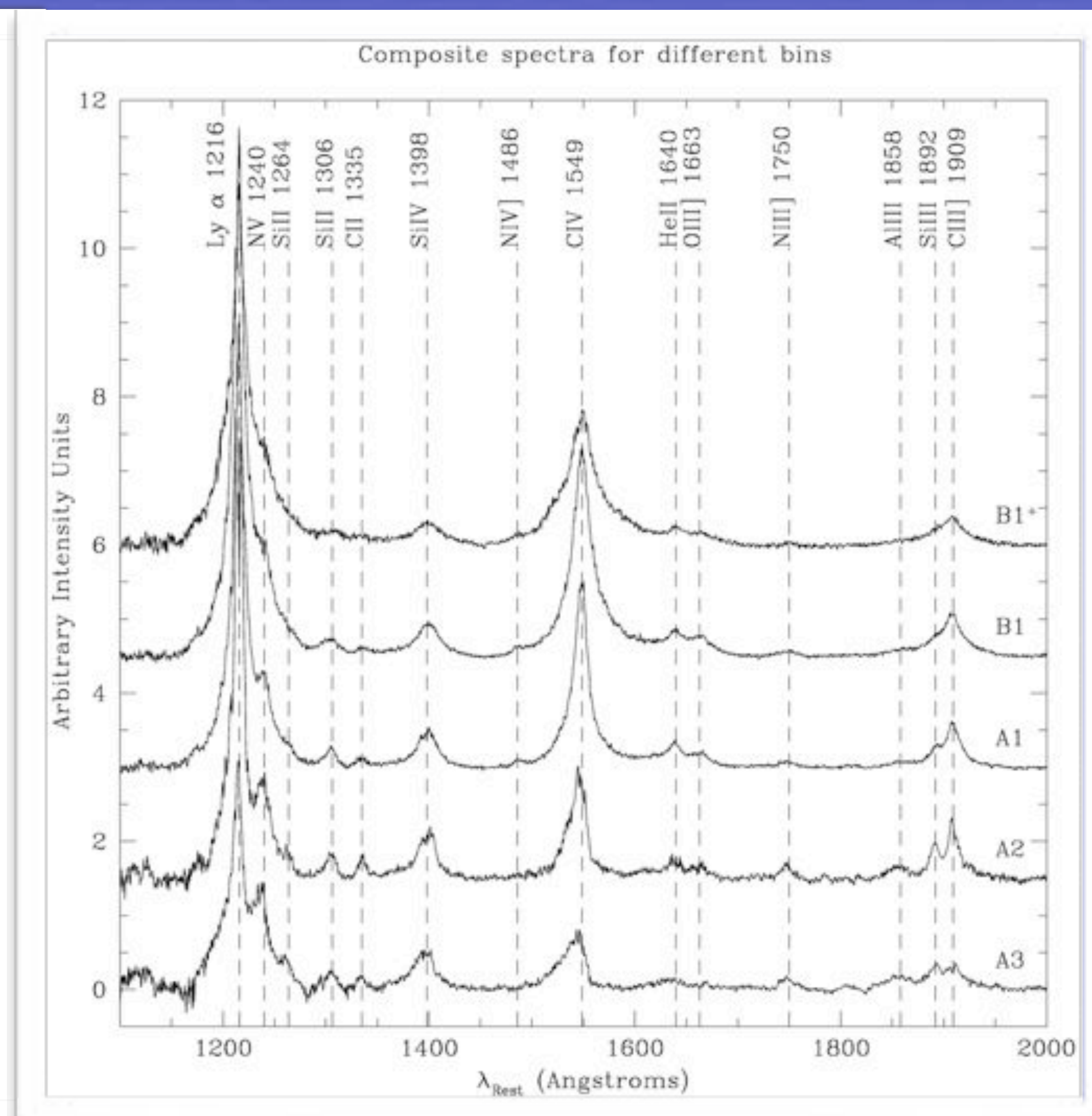

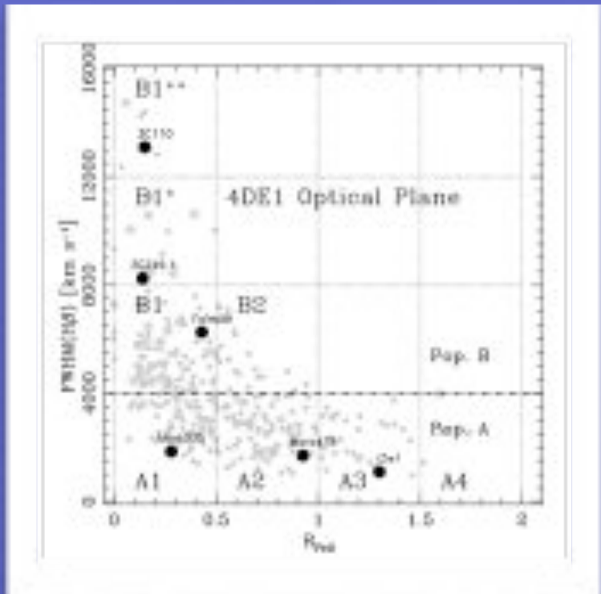


# The CIVλ1549 line profile

Modeled by a scaled Hβ profile + excess blueshifted emission: line broadening interpreted as due to virial motion + outflow

Marziani et al. 2010; cf Leighly 2000

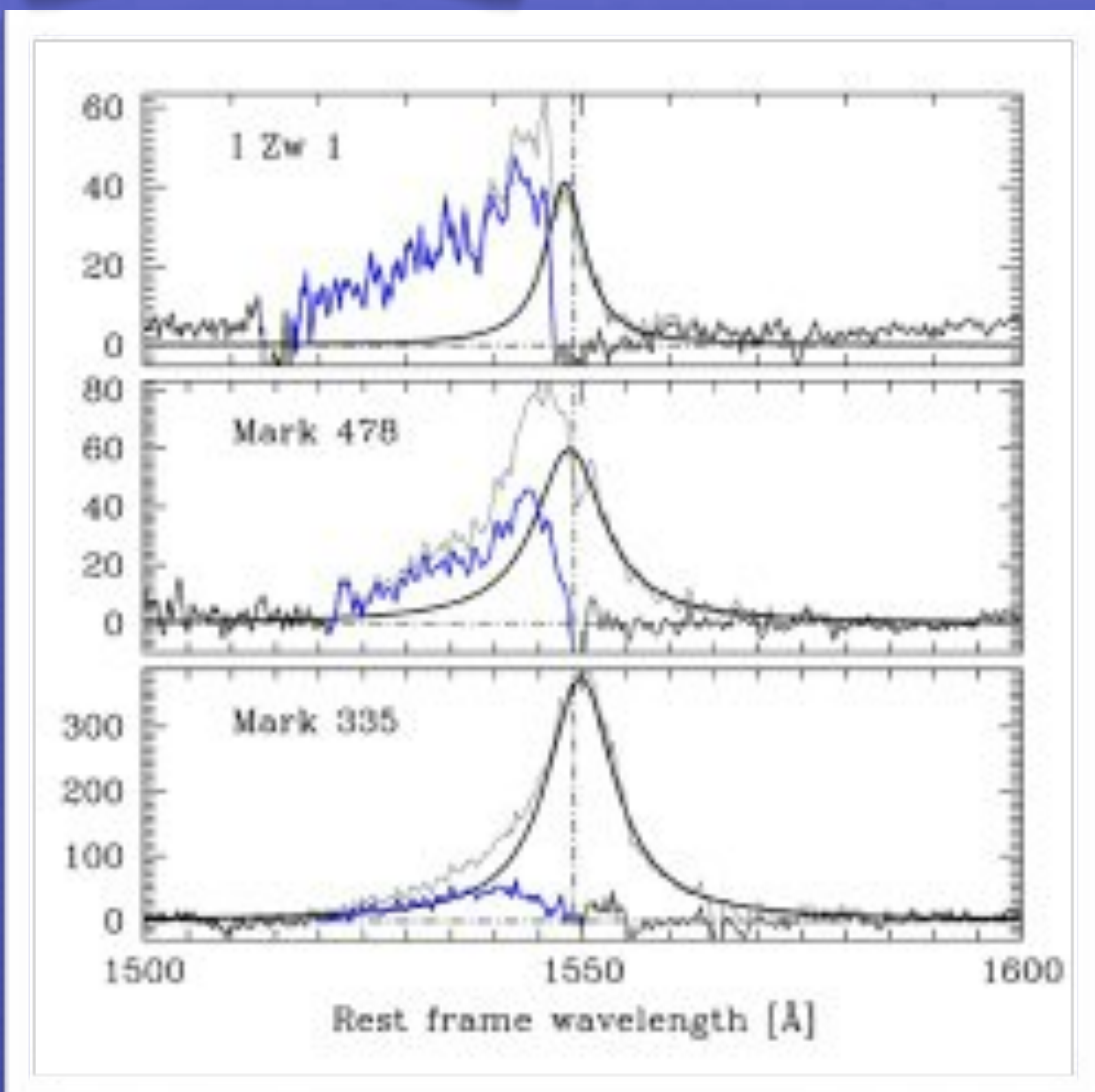


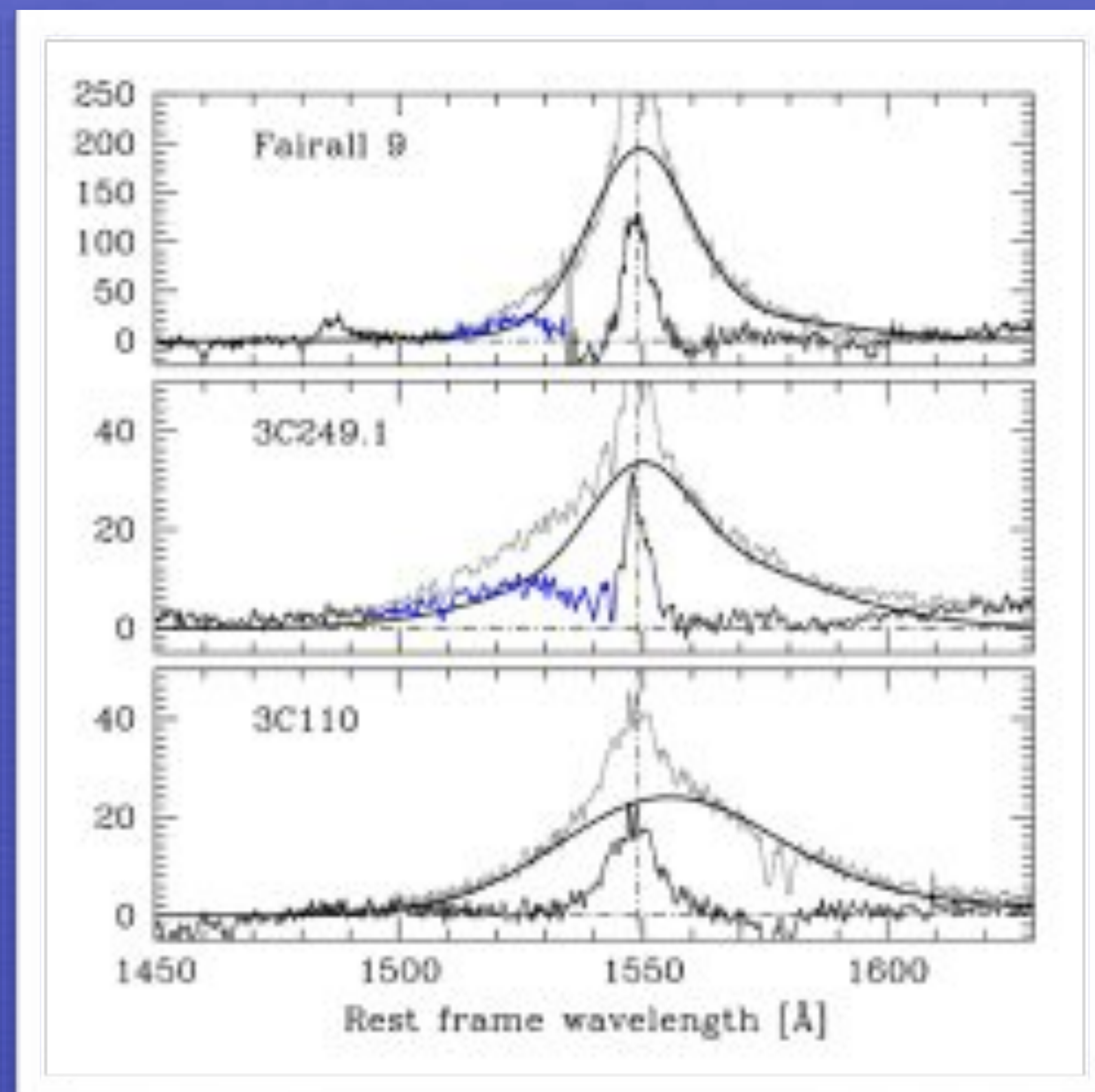

# The effect of including non virial components in black hole mass determination

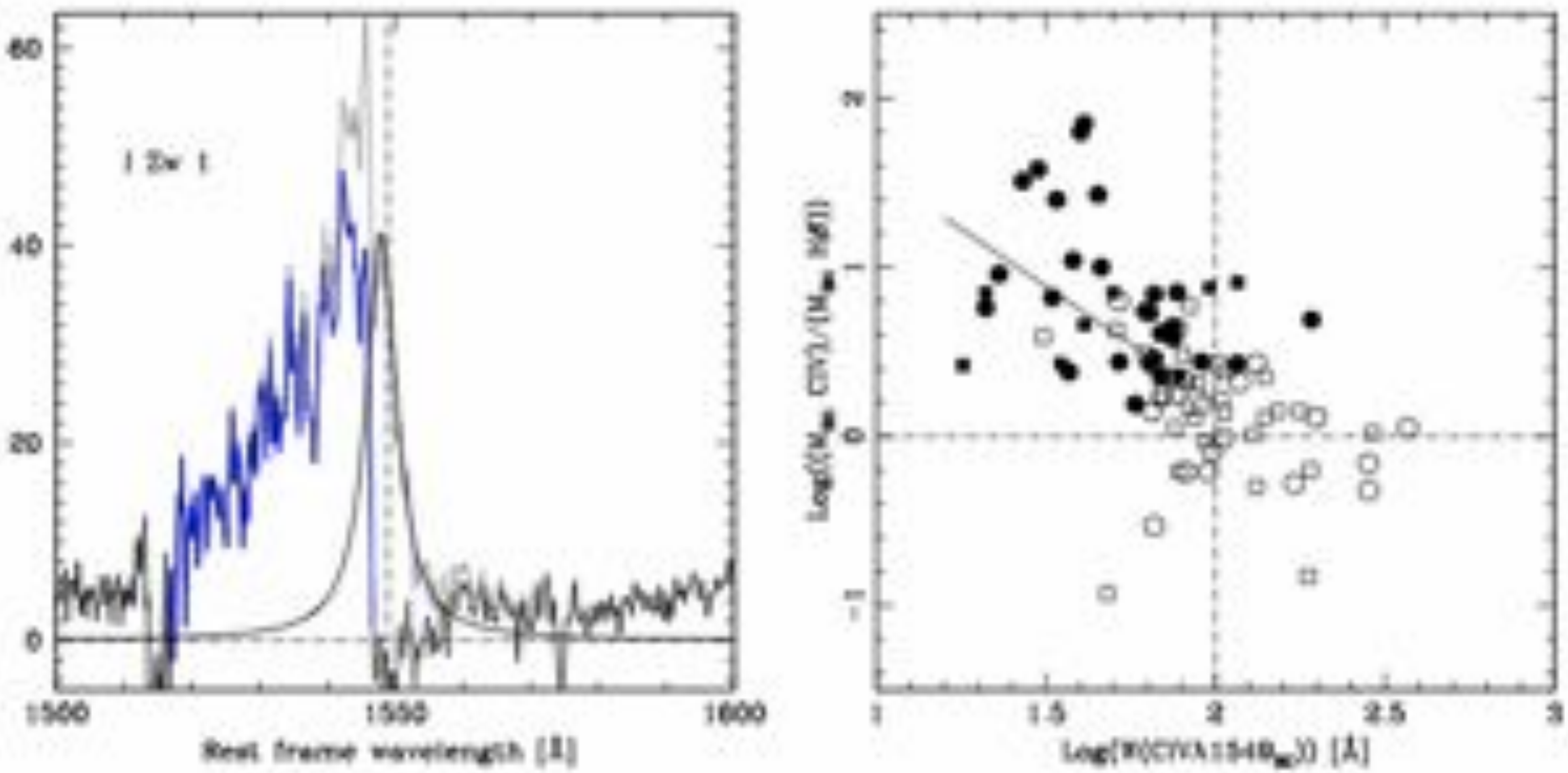


Sulentic et al. 2007; Marziani &  Sulentic 2012 and references therein

# UV spectral systematic changes along E1

Bachev et al. 2004

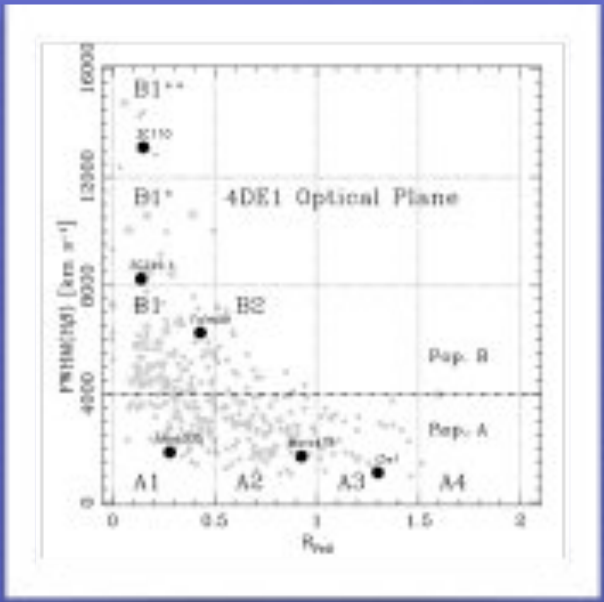


Along the sequence (A4 → B1++)

NVλ1240 ↘

AlIIIλ1860 ↘

CIII]λ1909 ↗

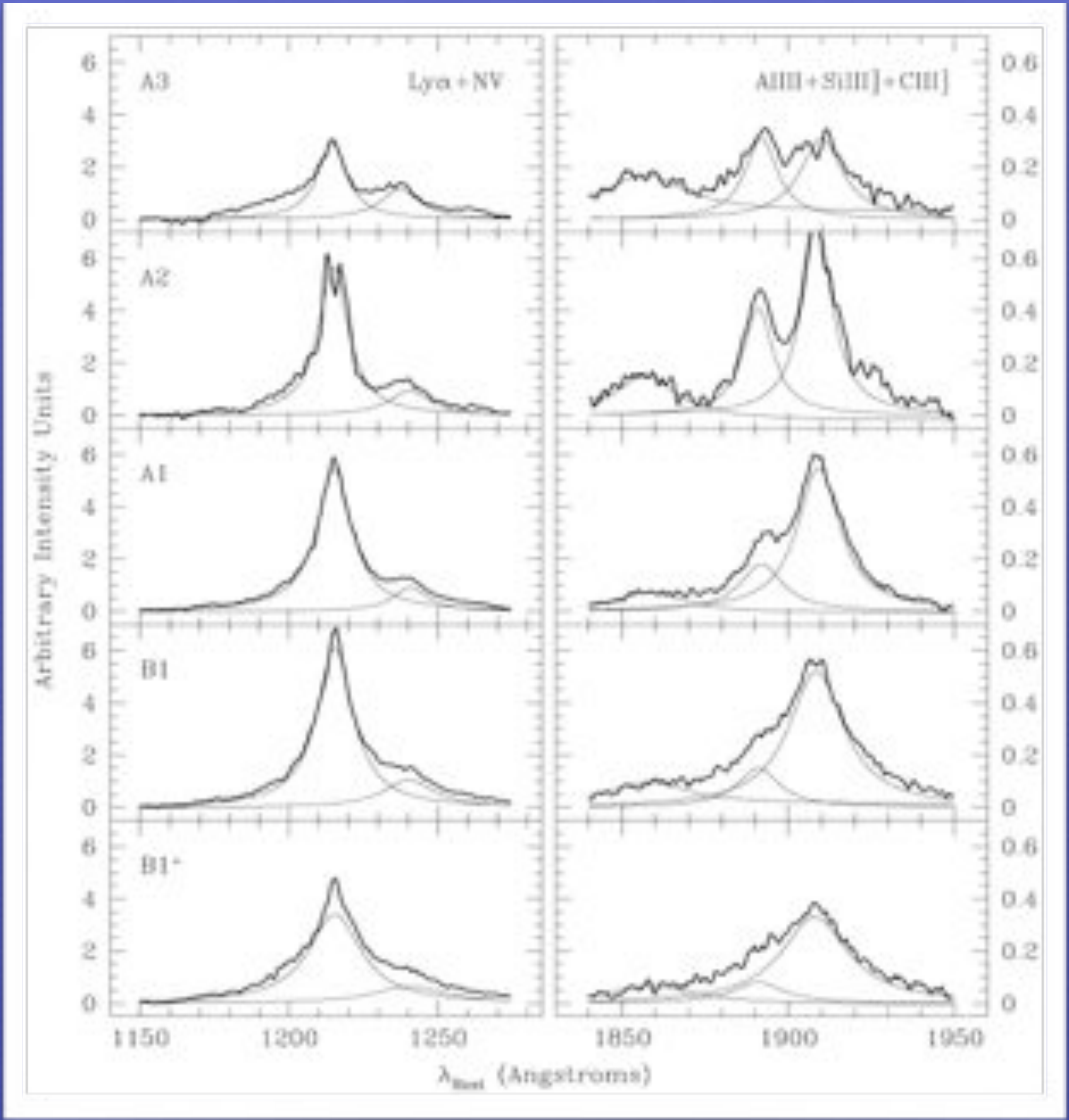

# Quasar diagnostics

TABLE 1
LINES IN THE 1350–2000 Å SPECTRAL RANGE

| Ion | $\lambda$ [Å] | $X$ [eV] | $E_l - E_u$ [eV] | Transition | $A_{ki}$ [$s^{-1}$] | $n_c$ [$cm^{-3}$] | Note |
|---|---|---|---|---|---|---|---|
| Si IV | 1393.755 | 45.20 | 0.000 - 8.896 | $^2P^o_{3/2} \rightarrow {}^2S_{1/2}$ | $8.80 \cdot 10^8$ | ··· | 1 |
| Si IV | 1402.770 | 45.20 | 0.000 - 8.839 | $^2P^o_{1/2} \rightarrow {}^2S_{1/2}$ | $8.63 \cdot 10^8$ | ··· | 1 |
| C IV | 1548.202 | 47.89 | 0.000 - 8.008 | $^2P^o_{3/2} \rightarrow {}^2S_{1/2}$ | $2.65 \cdot 10^8$ | ··· | 1 |
| C IV | 1550.774 | 47.89 | 0.000 - 7.995 | $^2P^o_{1/2} \rightarrow {}^2S_{1/2}$ | $2.64 \cdot 10^8$ | ··· | 1 |
| Si II | 1808.00 | 8.15 | 0.000 - 6.857 | $^2D^e_{3/2} \rightarrow {}^2P_{1/2}$ | $2.54 \cdot 10^6$ | ··· | 1 |
| Si II | 1816.92 | 8.15 | 0.036 - 6.859 | $^2D^e_{5/2} \rightarrow {}^2P_{3/2}$ | $2.65 \cdot 10^6$ | ··· | 1 |
| Al III | 1854.716 | 18.83 | 0.000 - 6.685 | $^2P^o_{3/2} \rightarrow {}^2S_{1/2}$ | $5.40 \cdot 10^8$ | ··· | 1 |
| Al III | 1862.790 | 18.83 | 0.000 - 6.656 | $^2P^o_{1/2} \rightarrow {}^2S_{1/2}$ | $5.33 \cdot 10^8$ | ··· | 1 |
| [Si III] | 1882.7 | 16.34 | 0.000 - 6.585 | $^3P^o_2 \rightarrow {}^1S_0$ | 0.012 | [illegible] | 1,2,3 |
| Si III] | 1892.03 | 16.34 | 0.000 - 6.553 | $^3P^o_1 \rightarrow {}^1S_0$ | 1670 | $2.1 \cdot 10^{11}$ | [illegible],5 |
| [C III] | 1906.7 | 24.38 | 0.000 - 6.502 | $^3P^o_2 \rightarrow {}^1S_0$ | 0.0052 | [illegible] | 1,2,6 |
| C III] | 1908.734 | 24.38 | 0.000 - 6.495 | $^3P^o_1 \rightarrow {}^1S_0$ | 114 | $1.4 \cdot 10^{10}$ | [illegible],4,5 |
| Fe III | 1914.066 | 16.18 | 3.727 - 10.200 | $z^7P^o_3 \rightarrow a^7S_3$ | $6.6 \cdot 10^8$ | ··· | 7 |

NOTE. — All wavelengths are in vacuum. (1) Ralchenko, Yu., Kramida, A.E., Reader, J., and NIST ASD Team (2008). NIST Atomic Spectra Database (version 3.1.5). Available at: http://physics.nist.gov/asd3. 2: Feibelman & Aller (1987). 3: $n_c$ computed following Shaw & Dufour (1995). 4: Morton (1991). 5: Feldman (1992). 6: Zheng (1988). 7: Wavelength and $A_{ki}$ from Ekberg (1993), energy levels from Edlén and Swings (1942).

CIV (Al III, Si IV,NV)

C III] (Si III])

Si II

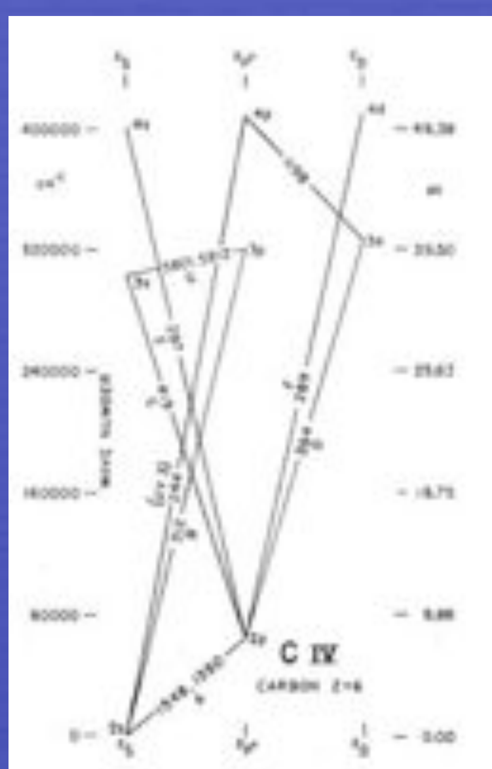


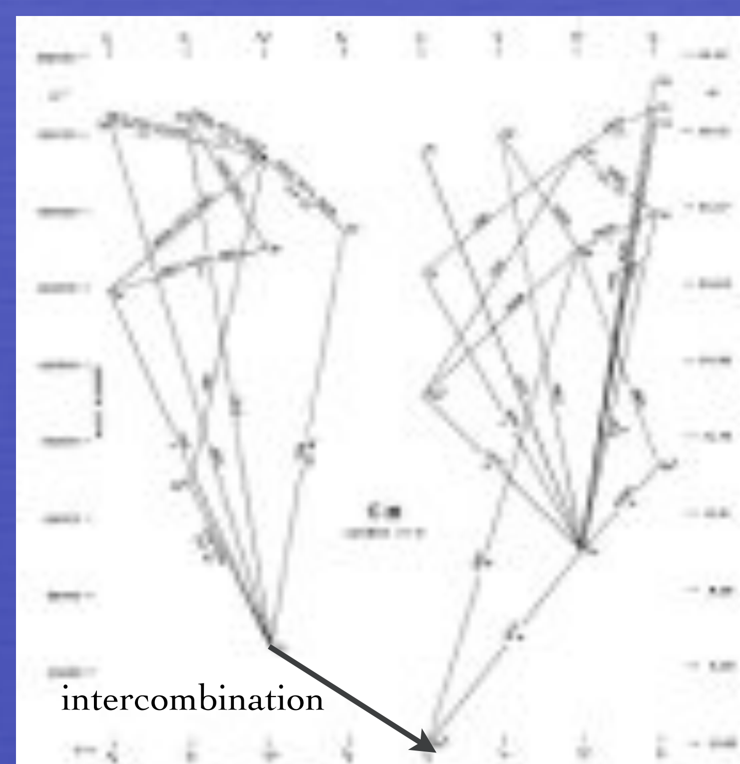


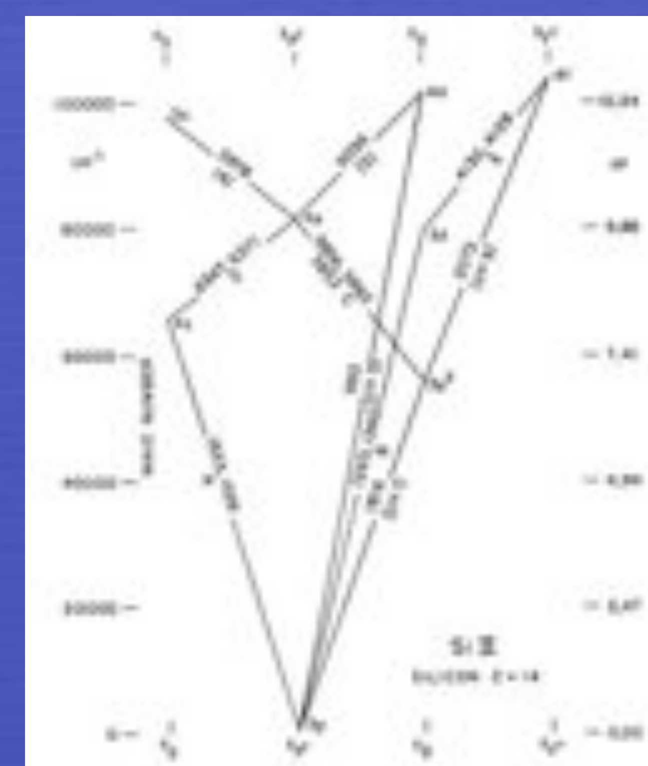

# Diagnostic Intensity Ratios

(SIV+OIV])λ1400/Si III] λ1892
Si II 1814/Si III] λ1892

*independent on metallicity*
*sensitive to ionization*

CIV λ1549/(Si IV+OIV])λ1400

*sensitive to metallicity*

Al III λ1860/Si III] λ1892
Si III] λ1892/CIII] λ1909

*sensitive to density*

C IV λ1549/Al III λ1860
C IV λ1549/Si III] λ1892

*sensitive to ionization*
*dependent on metallicity*

NVλ1240/CIV λ1549
NVλ1240/HeIIλ1640

*sensitive to metallicity*

+ many others involving fainter lines like NIII]λ1750
(but caution with intercombination lines!)

# Behavior of line ratios in the plane ionization parameter vs. density

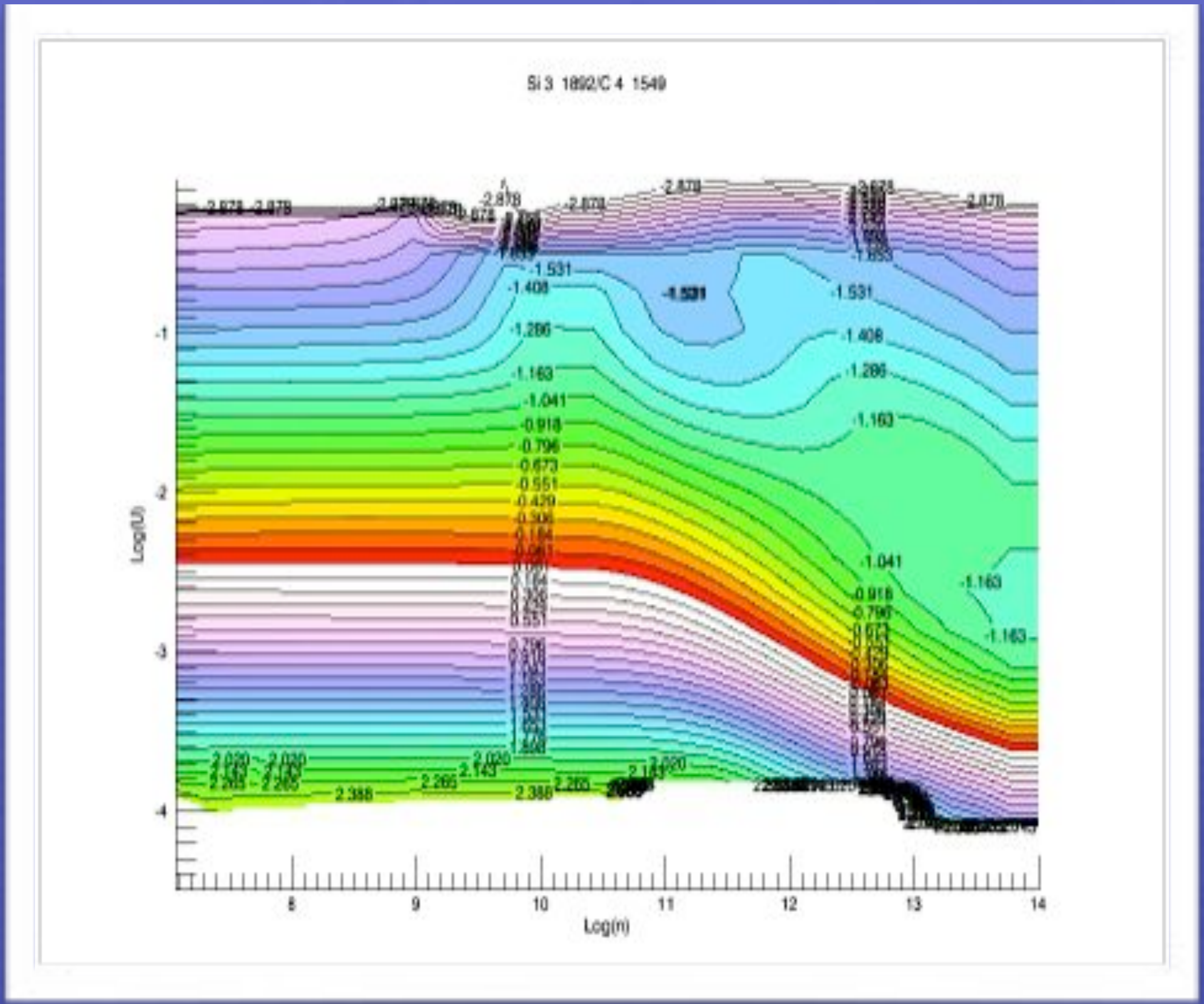


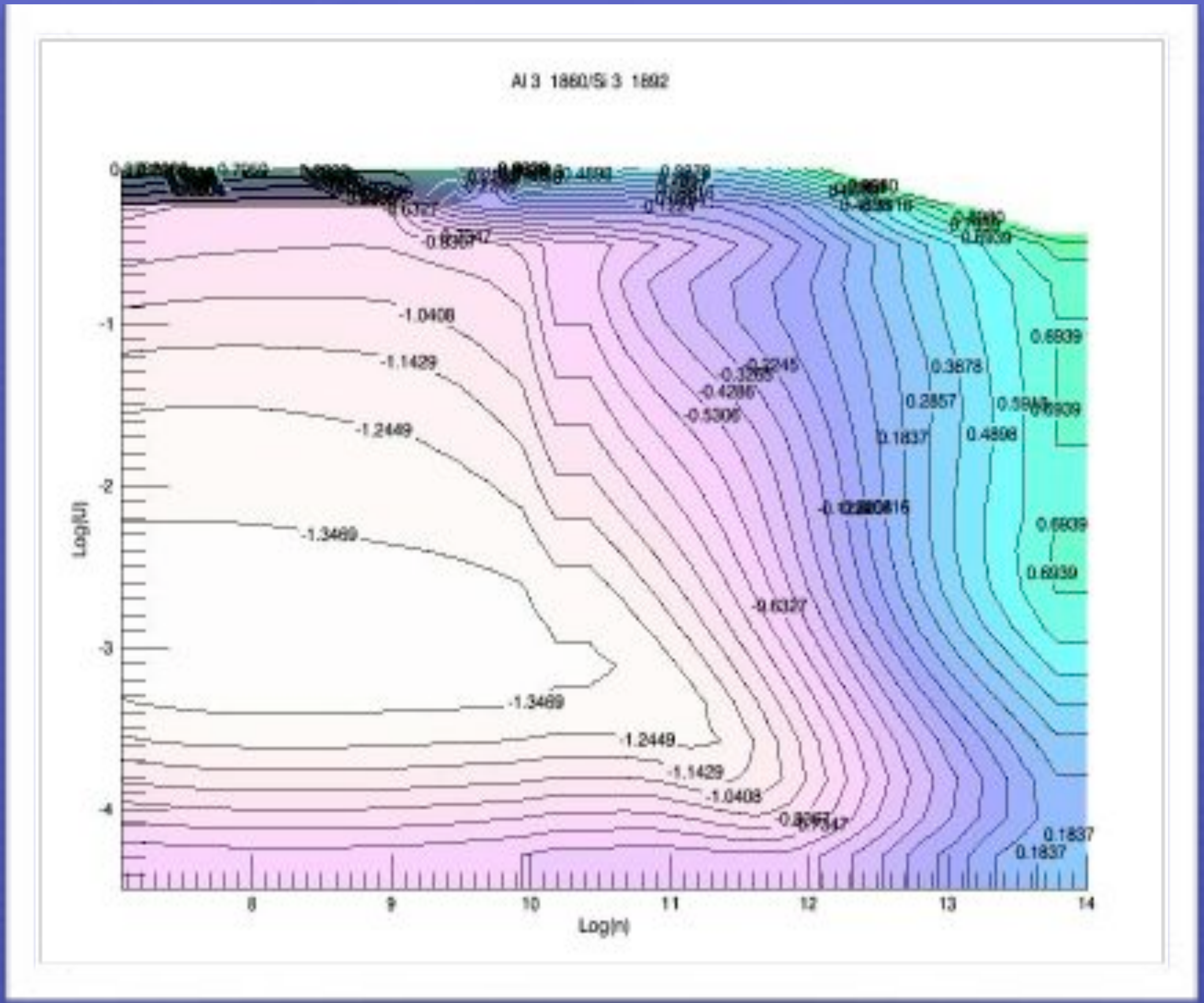


## Maps built on an array of 571 photoionization models

Cloudy 08.00 array of simulations (Ferland et al. 2013): constant density, U, solar abundances and standard quasar continuum

# A diagnostic of ionizing photon flux

## analysis of sources with HST/FOS observations and Hβ reverberation mapping

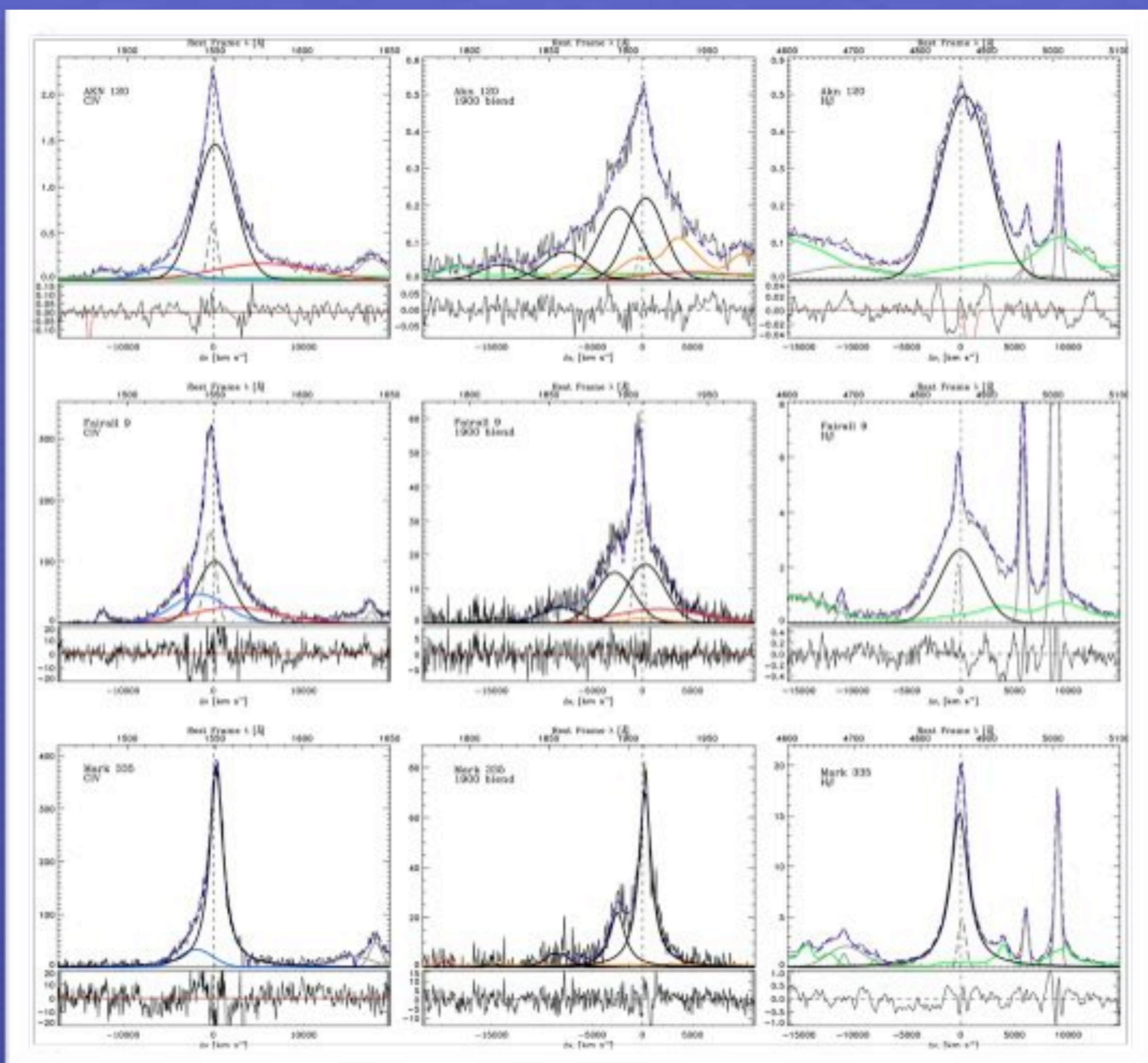

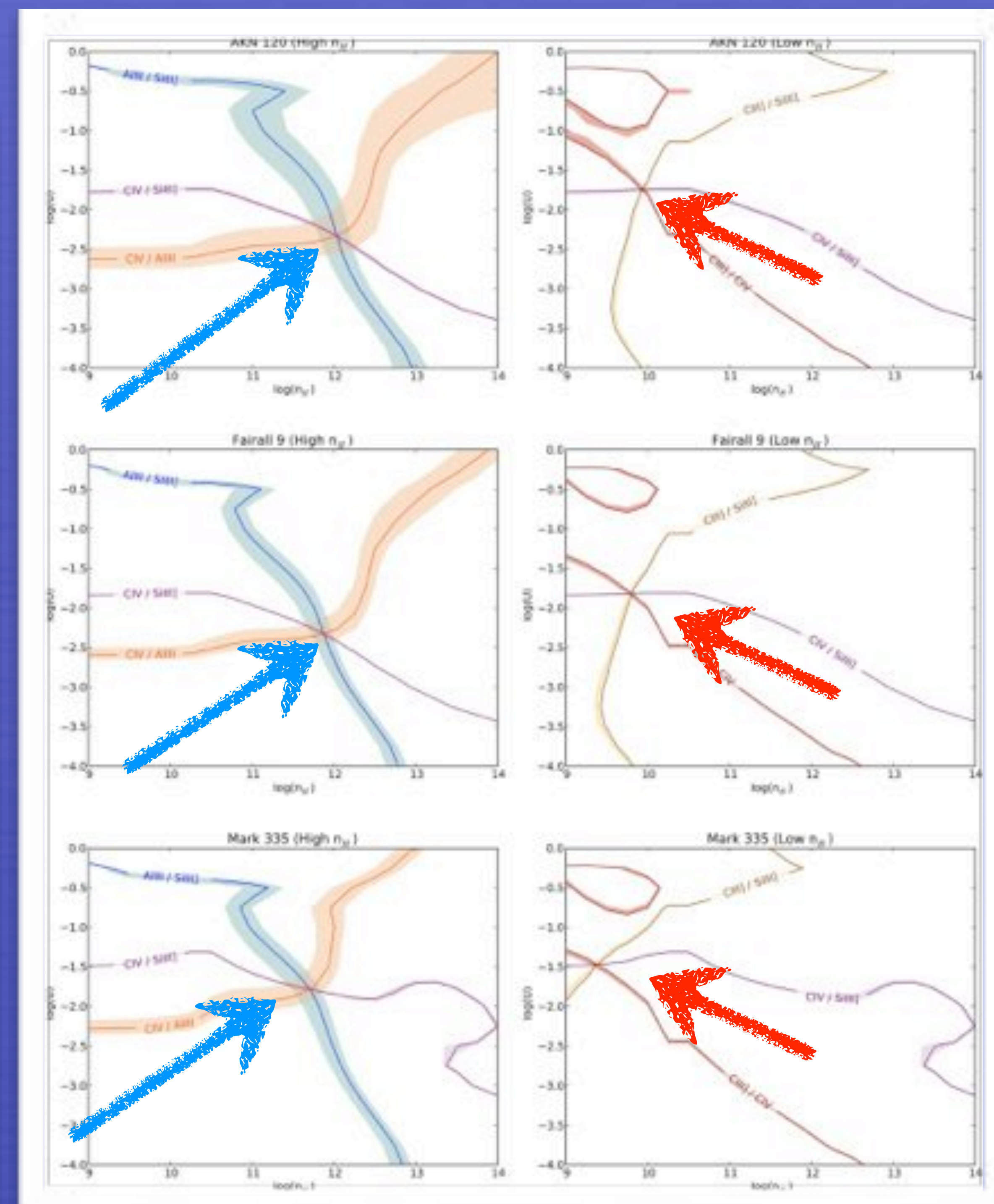

# "Photoionization" $r_{\mathrm{BLR}}$ and black hole mass

ionization parameter: ratio between photon and electron density

$$U = \frac{\int_{\nu_0}^{+\infty} \frac{L_\nu}{h\nu} d\nu}{4\pi r_{\mathrm{BLR}}^2 n_{\mathrm{e}} c}$$

emitting region radius

$$r_{\mathrm{BLR}} = \left( \frac{\int_{\nu_0}^{+\infty} \frac{L_\nu}{h\nu} d\nu}{4\pi U n_{\mathrm{e}} c} \right)^{\frac{1}{2}}$$

$$r_{\mathrm{BLR}} = \underbrace{\frac{1}{(4\pi c)^{\frac{1}{2}}}}_{\text{const.}} \underbrace{(U n_{\mathrm{e}})^{-\frac{1}{2}}}_{\text{diagnostics}} \left( \underbrace{\int_{\nu_0}^{+\infty} \frac{L_\nu}{h\nu} d\nu}_{\#\ \text{ionizing photons}} \right)^{\frac{1}{2}}$$

Padovani et al. 1990; Wandel et al. 1999, Negrete et al. 2012, c.f. Dibai 1977 and Bochkarev & Gaskell 2009

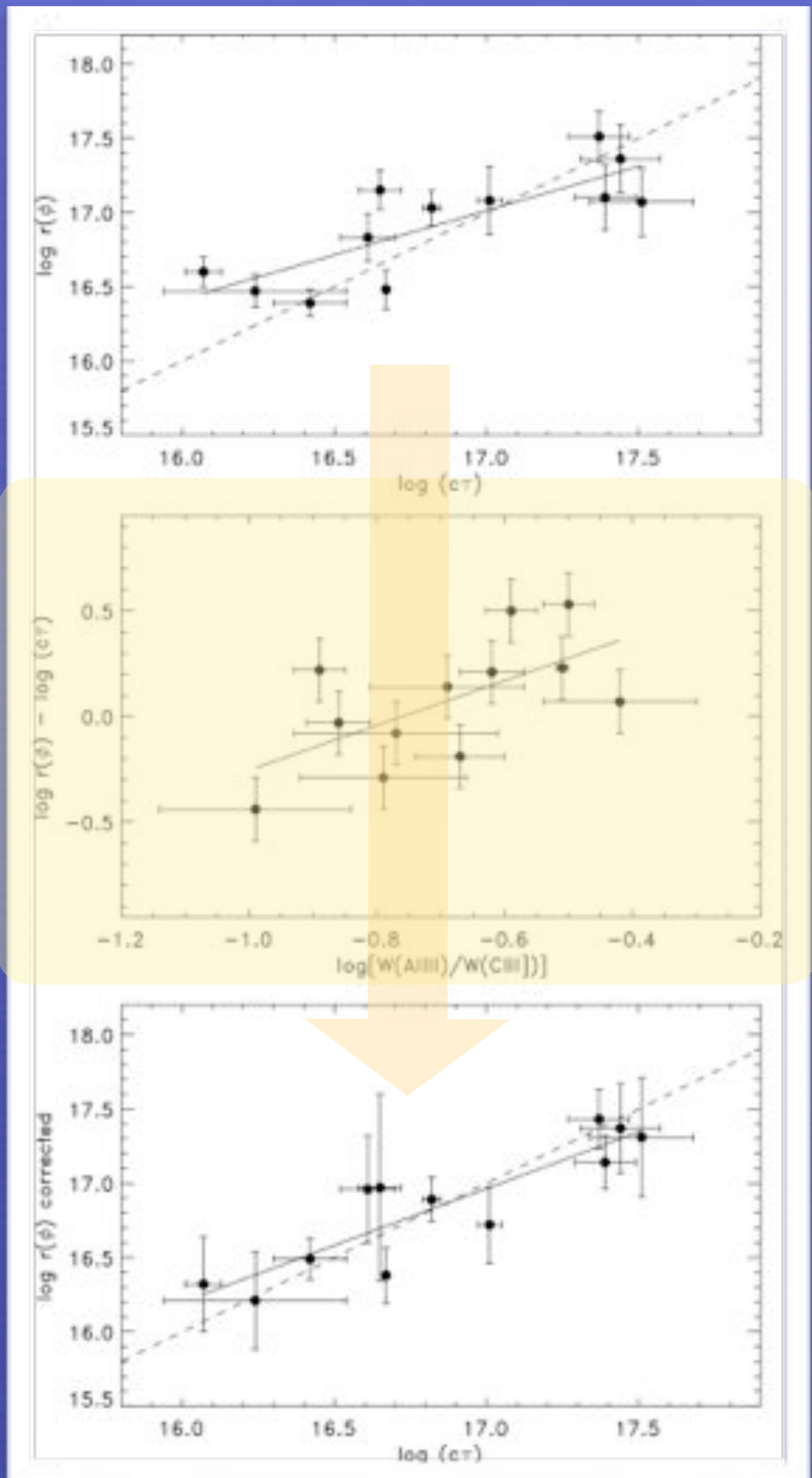


The combined Al III $\lambda$1860/Si III] $\lambda$1892 and C IV $\lambda$1549/Si III]$\lambda$1892 ratios are estimators of the ionizing photon flux: $r_{\mathrm{BLR}}$ is in agreement with c$\tau$ of H$\beta$ from reverberation mapping: rms ≈ 0.2 dex. (Negrete et al. 2013)

A correction is needed because of ionization and density gradients within the BLR.

Profiles allow for reliable computations of the virial black hole mass:

$$M_{\mathrm{BH}} = \frac{f r_{\mathrm{BLR}} (\mathrm{FWHM})^2}{G}$$

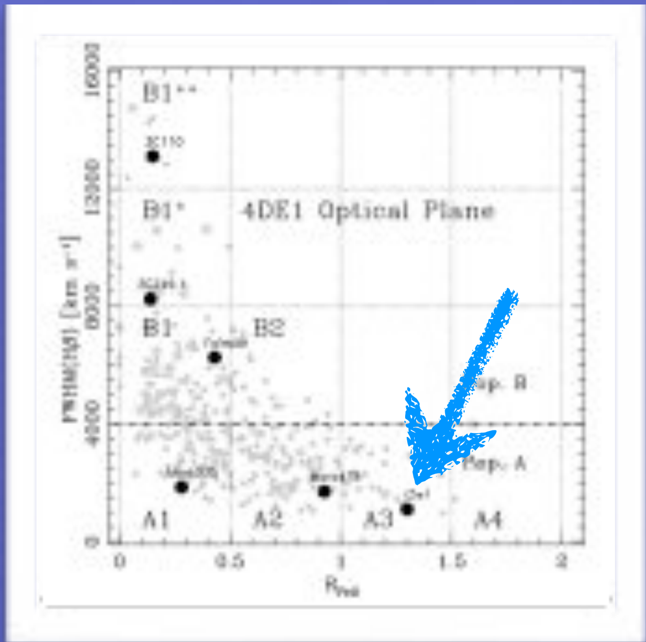


# Extreme A sources

young/rejuvenated quasars, revealed at both high and low luminosity, radiating at high Eddington ratio, 10% of in optically selected samples

Weak CIII]λ1909 and OIV]λ1402

(Dultzin et al. 2011; Negrete et al. 2012)

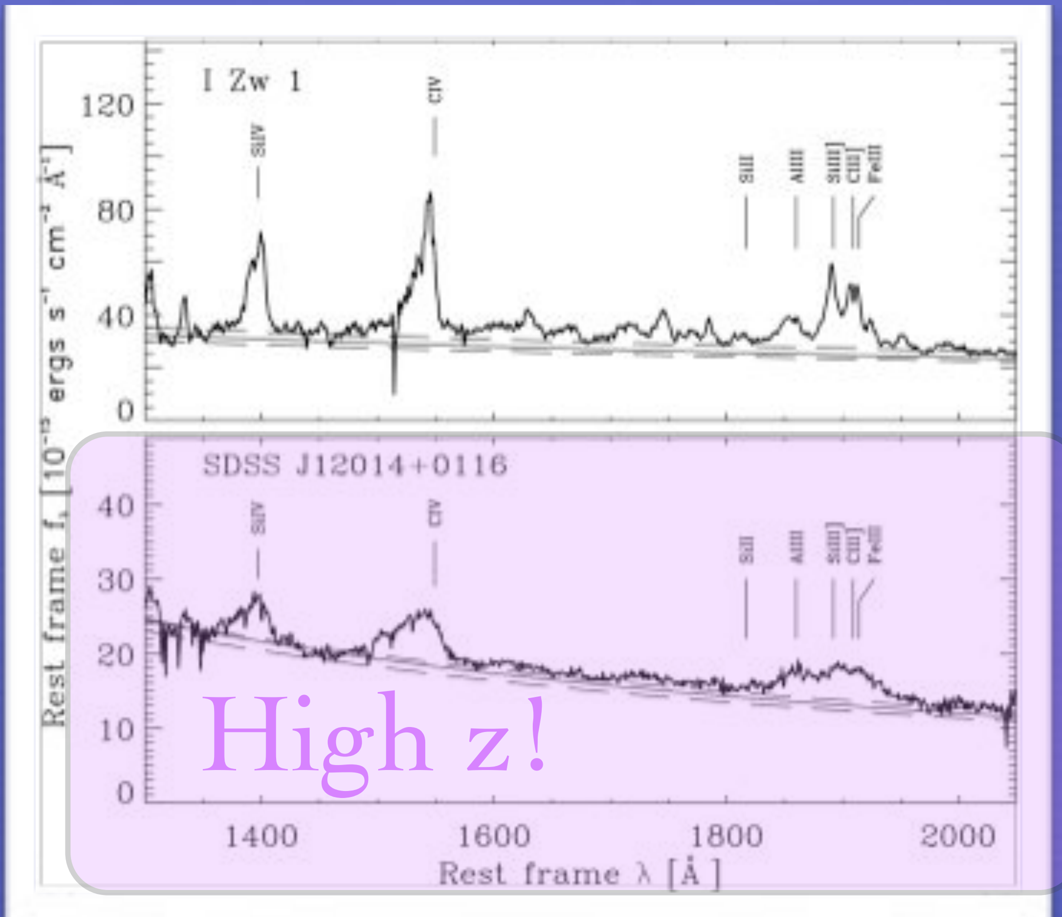


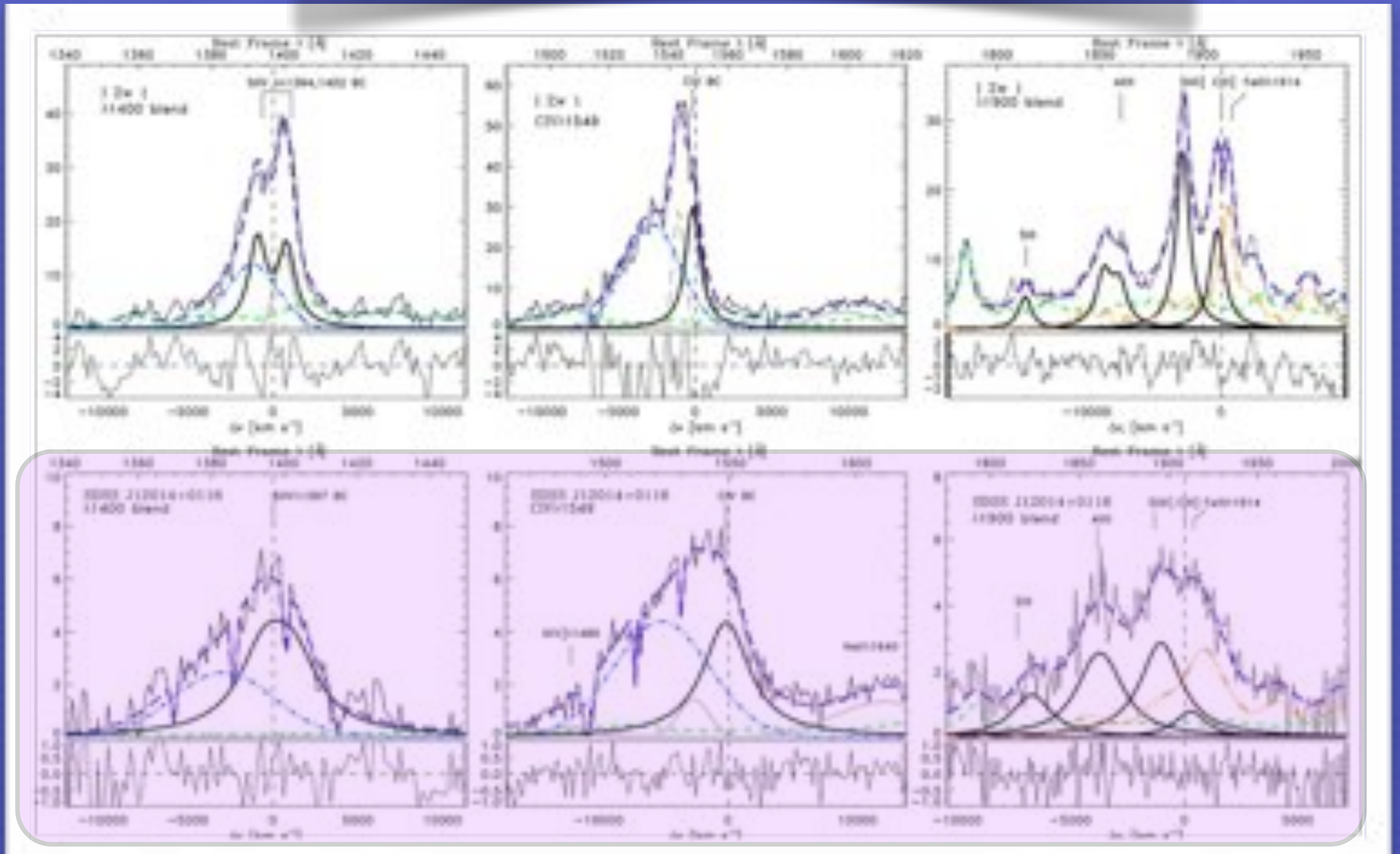

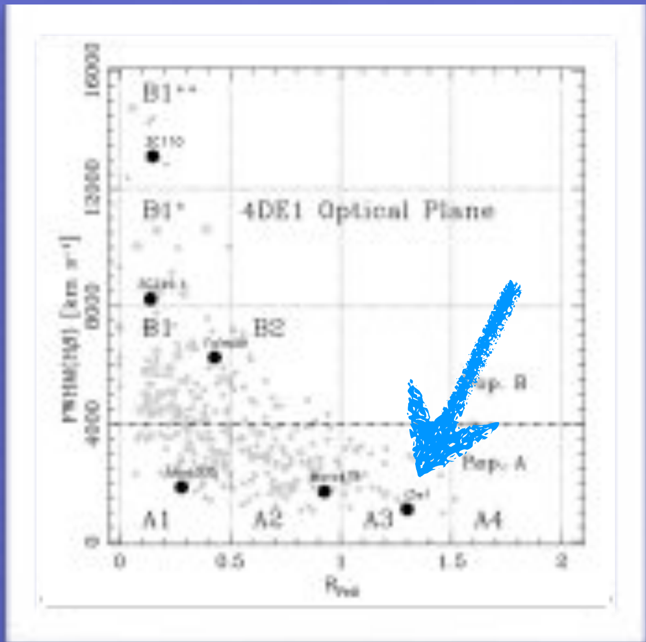


# Extreme A sources

Physical conditions: high density, low ionization and high metallicity

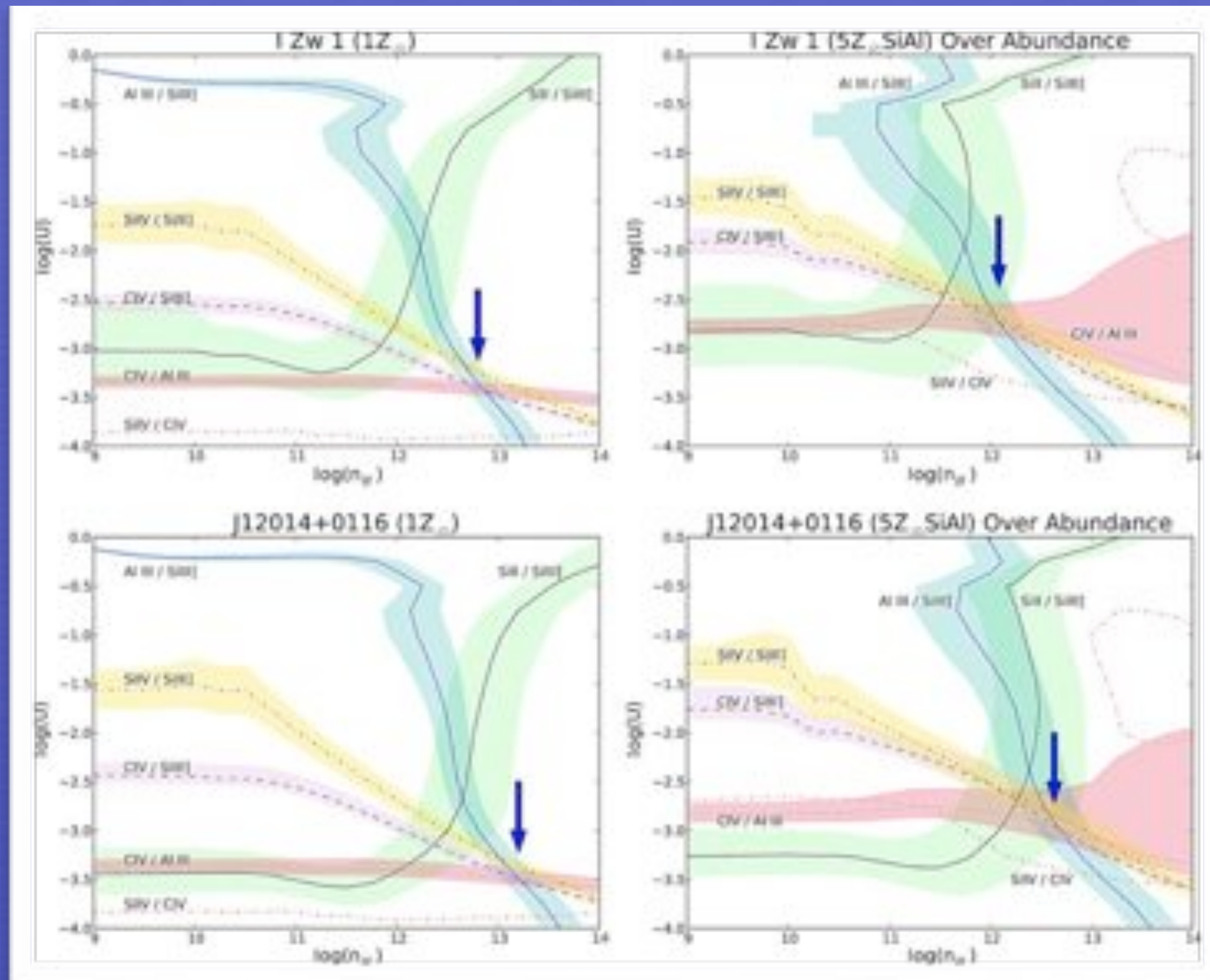

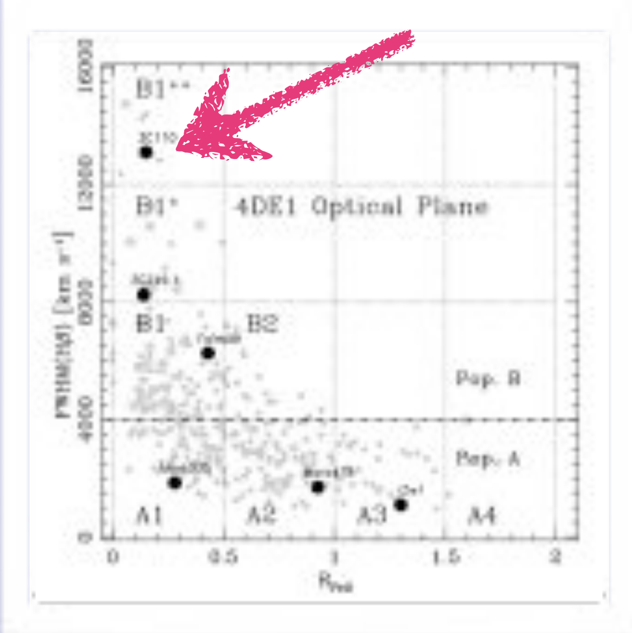


# Extreme B sources

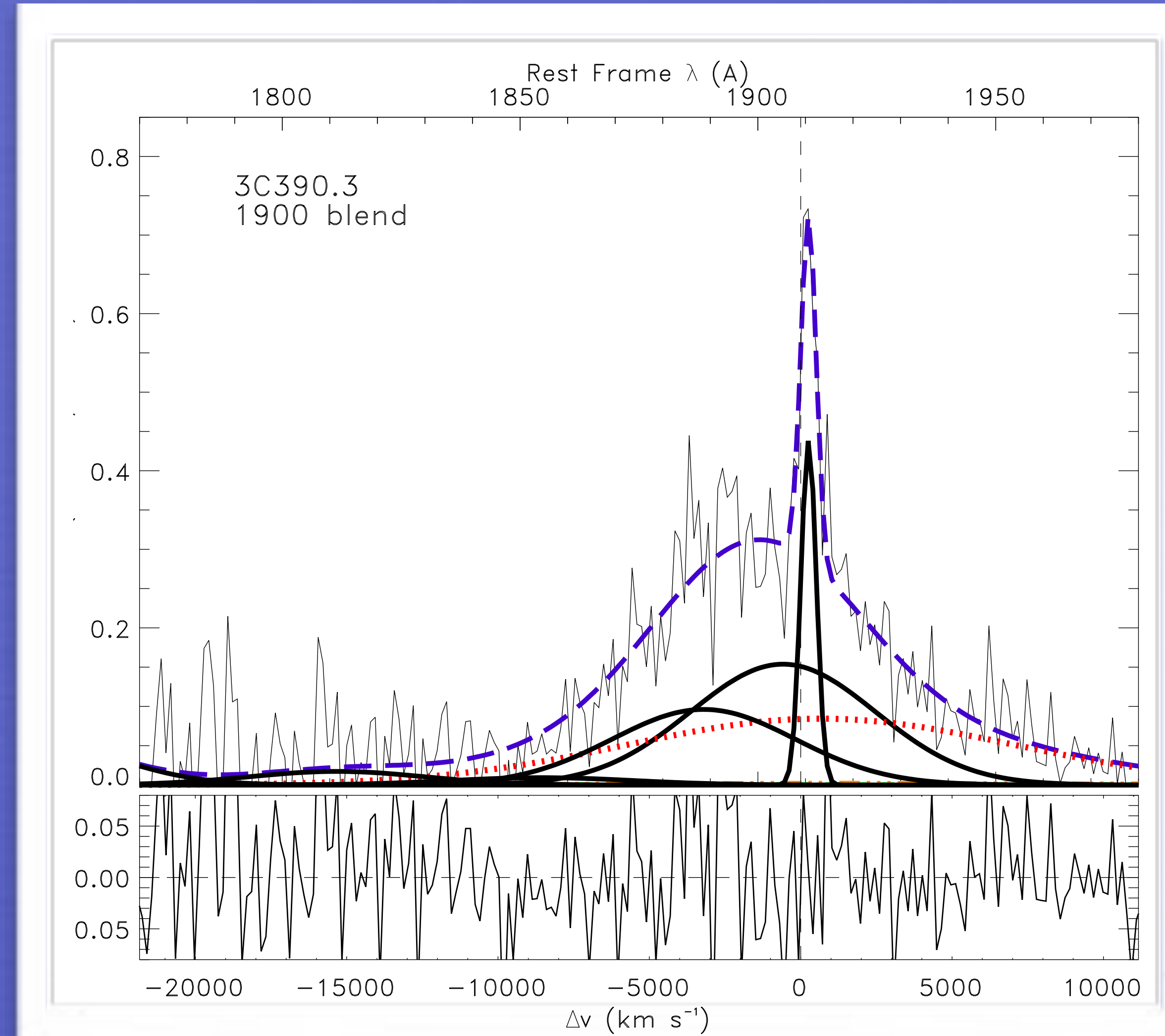


At the other end of E1: almost no Al III λ1860, prominent CIII] λ1909: lower density and high ionization

Physical conditions are more complex for most AGNs along the sequence due to the well known "stratification" of ionization.

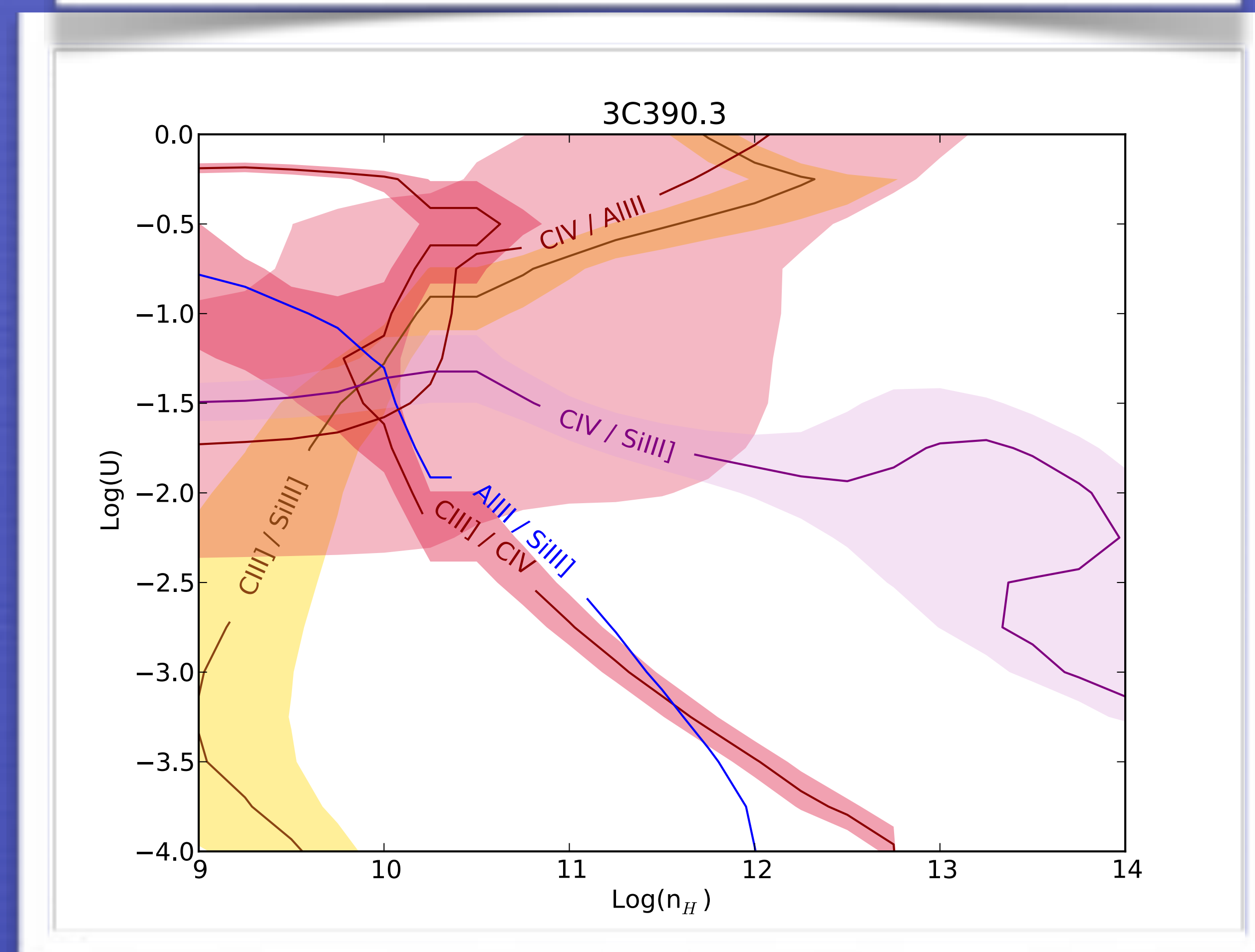

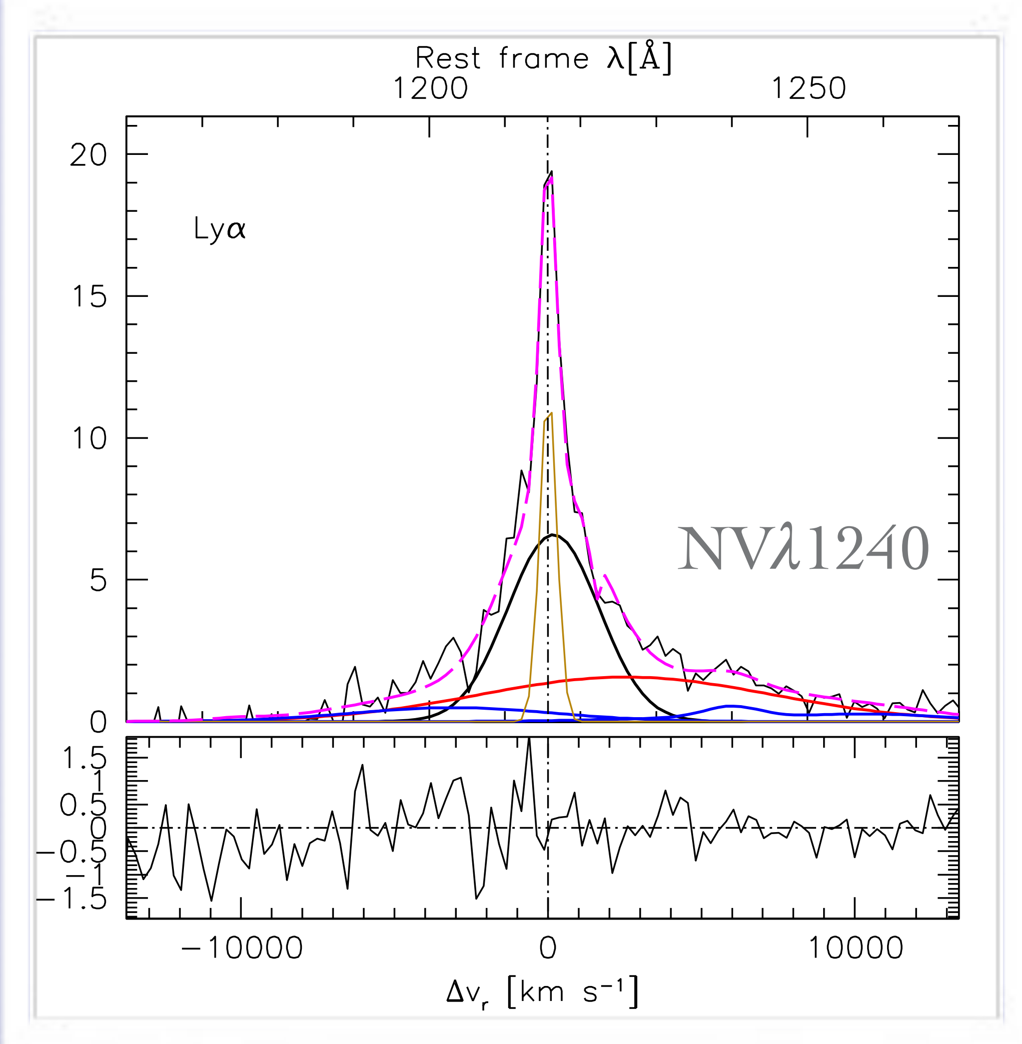


Sulentic et al. in preparation

# Chemical composition

A reliable analysis requires high dispersion and high S/N

Still many open issues on chemical enrichment of low-*z* quasars, in part due to lack of suitable data.

Hamann & Ferland 1999

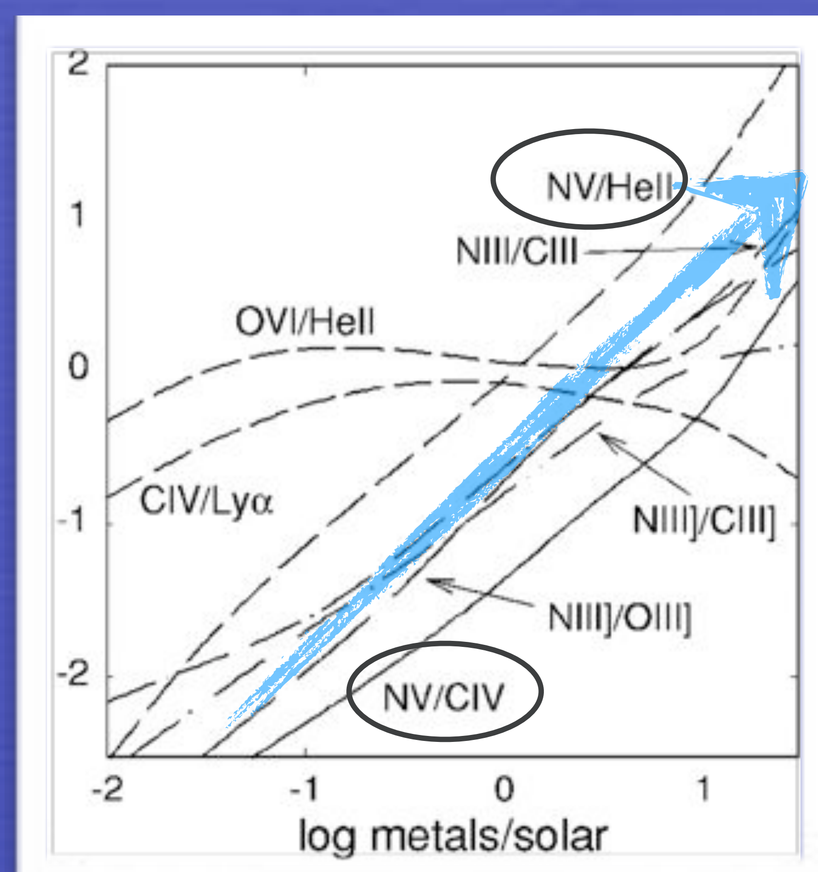


Shin et al. 2013

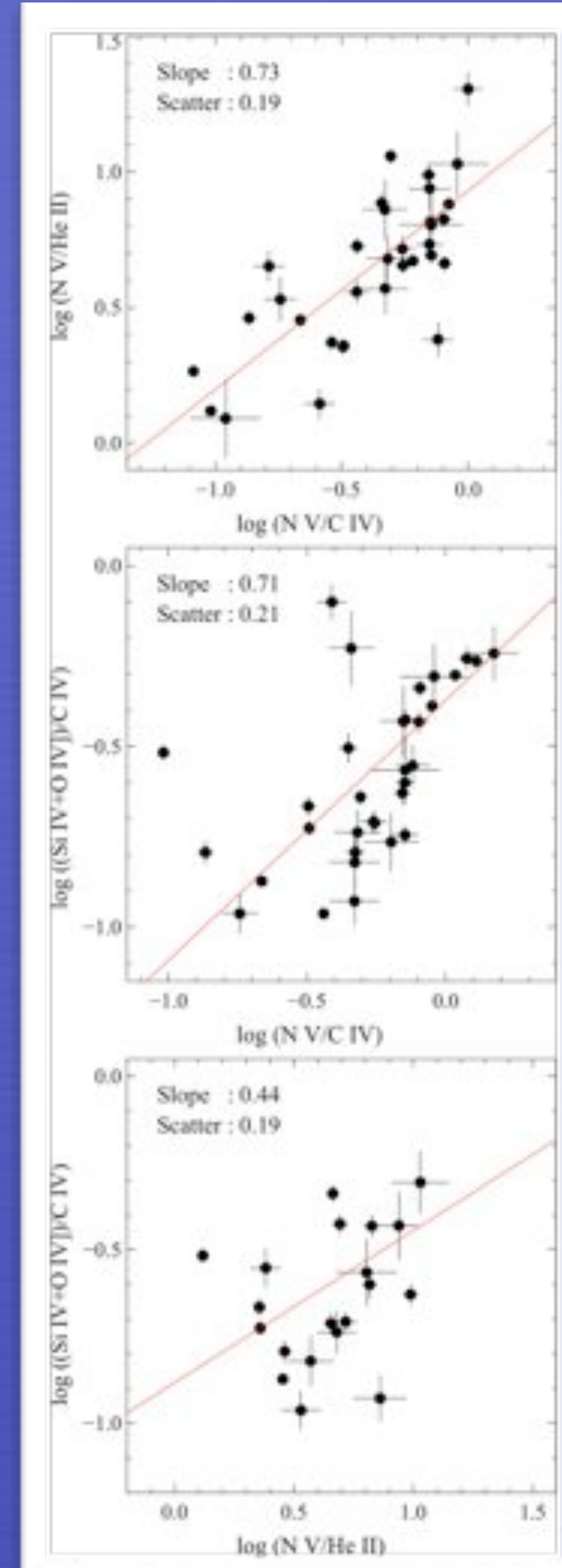

# MAST inspection

## 1) Palomar Green quasars

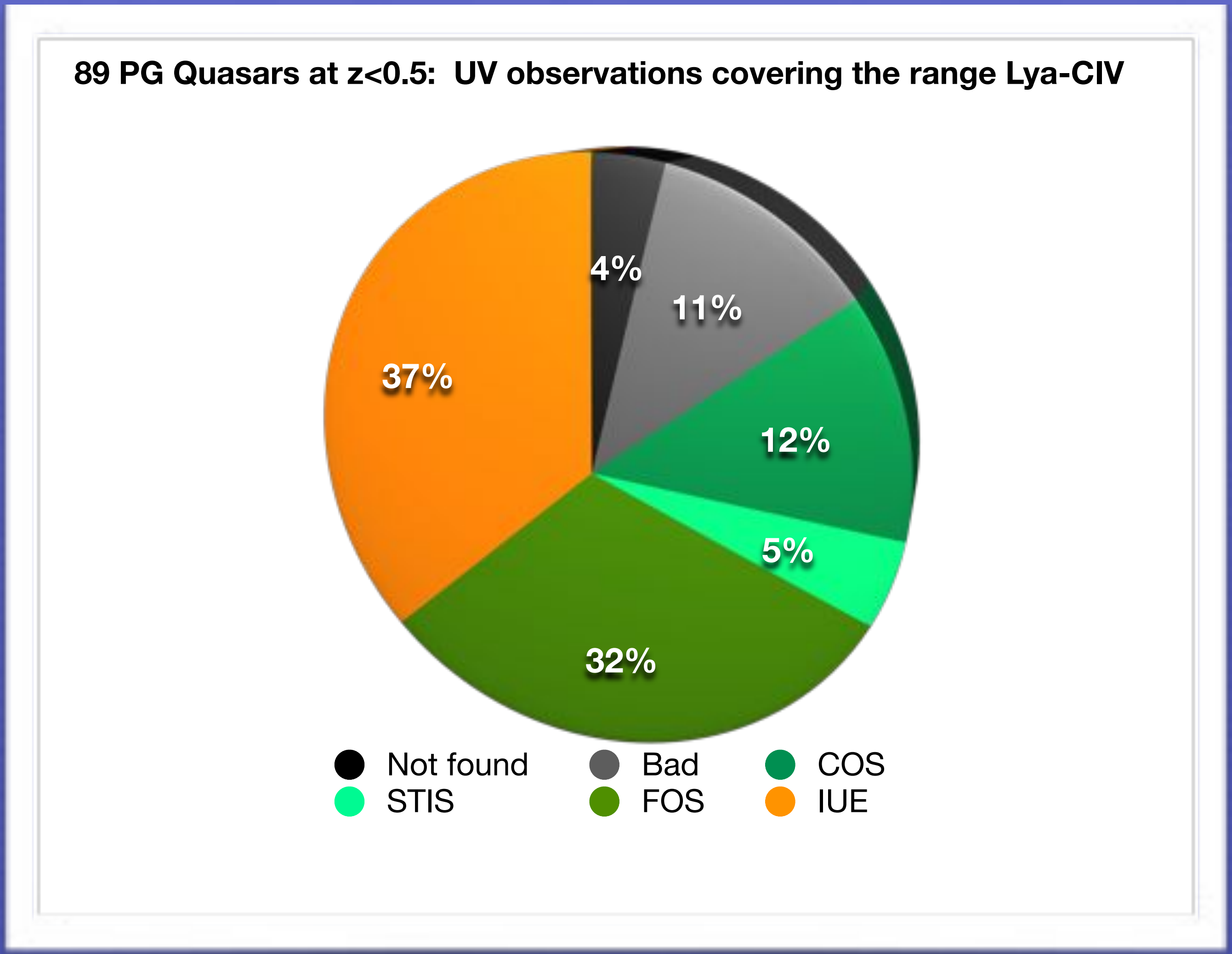


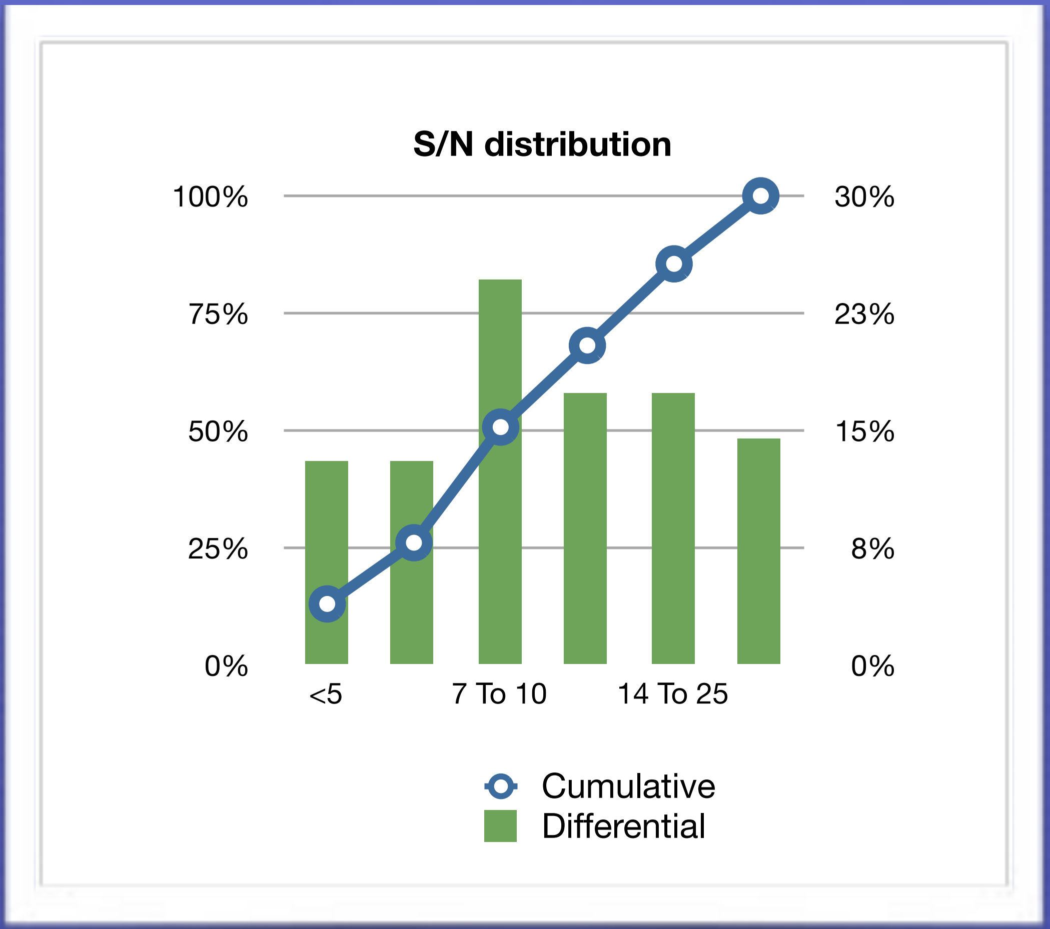


Data from Shin et al. 2013

Only 50% of PG quasars covered by HST observations

2) Of 600 type-1 AGNs detected at 6cm with $m<19$ and $z<0.90$ only a minority have HST spectroscopic observations

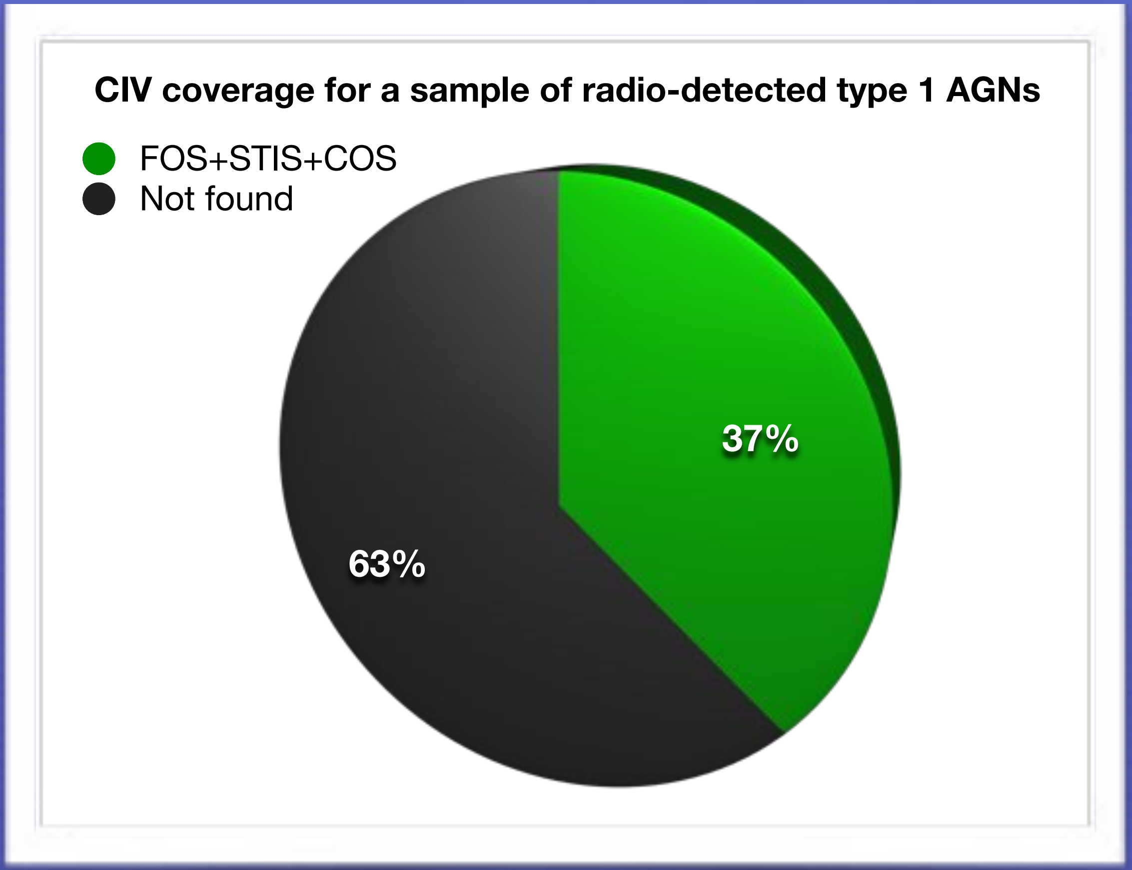


3) only a handful of AGNs monitored for reverberation mapping in the UV

# Conclusions

Rest frame UV emission lines make it possible to derive quasar physical parameters that lead to emitting region radius, black hole mass, Eddington ratio,  etc.

The Eigenvector 1 sequence  allows to  identify sources that are physically and structurally different.

Archives from past /present space missions are extremely valuable  but much is still needed in terms of population coverage and data quality.